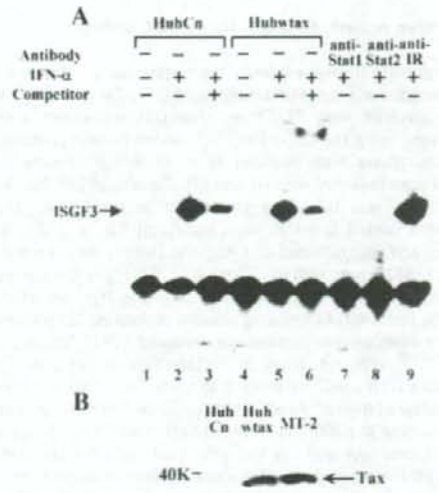

Fig. 2. Tax does not affect the formation of ISGF3 complex on ISRE promoter. (A) HuhCn or Huhwtax cells were treated in the absence or presence of 500 IU/ml of human IFN-α for 30 min. Nuclear extracts were prepared for EMSA analysis using labeled ISRE probe. In lanes 3 and 6, 50-fold molar excess of unlabeled ISRE competitor were included. In lanes 7–9, nuclear extracts were pre-incubated with the antibodies against STAT1, STAT2 or irrelevant β-actin (anti-IR) for 30 min prior to the addition of labeled probe. (B) Stable expression of Tax protein in Huhwtax cells was confirmed by Western blot analysis. Solid arrow indicates the signals of Tax protein.

α signaling without derailing the events involved in the formation of DNA-binding ISGF3 complex.

Tax represses transactivation function of STAT2

The results presented above imply that Tax averts IFN-α function via a mechanism other than inhibiting the activation and/or nuclear translocation of ISGF3 components. It is known that the C terminus of STAT2 serves as a transcriptional activation (TA) domain, which is essential for ISGF3 function. We next examined whether Tax could inhibit the transactivation function of STAT2. To this end, we constructed a vector pGAL4-Stat2(TA) by fusing the GAL4 DNA binding domain with the C-terminal 181 residues-coding region of STAT2. Expression of reporter gene from pGAL4-luc vector in HeLa cells was significantly induced by cotransfection with pGAL4-Stat2 (TA), but not by pGAL4-Stat2(TA)Δ with C-terminal 83 amino acids deleted, confirming the transactivation potential of the C terminus of STAT2 (Fig. 3). Importantly, cotransfection with Tax-expressing plasmid markedly inhibited the GAL4-Stat2(TA) transactivation activity, resulting in an approximately five- to six-fold lower luciferase expression when compared with the transfection in the absence of Tax. In contrast, the activation of the transcription from pGAL-luc by GAL4-VP16, which contains the activation domain of VP16 instead of Stat2 in GAL4-Stat2(TA), was not obviously affected by Tax protein, indicating that Tax-mediated inhibition of STAT2 transactivation is not due to an impairment of the general transcription machinery in Tax-expressing cells. Additionally, this result further excluded the possibility that Tax-mediated inhibition of ISGF3-directed transcription was attributable to the perturbation of events such as nuclear translocation because both GAL4-Stat2(TA) and GAL4-VP16 utilizes the same nuclear localization signal of GAL4. Taken together, these results suggest that Tax protein inhibits IFN-α signaling via repressing STAT2 transactivation.

Tax down-modulates IFN-α signaling by competitive binding to CBP/p300 coactivator

It has been demonstrated that STAT2 and STAT2-containing ISGF3 function in transcriptional activation partly through recruitment of CBP/p300 (Bhattacharya et al., 1996). Likewise, Tax also utilizes CBP/p300 for implementing its transcriptional activation competence, and moreover, Tax has been shown to inhibit CBP/p300-mediated transcription by competitive usage of the coactivator. Accordingly, a possible mechanism for Tax-mediated inhibition of IFN-α-activated ISGF3 transactivation is through binding to CBP/p300 in competition with STAT2. If it is true, the binding ability of Tax to CBP/p300 should be crucial for its repression of ISGF3 transactivation. To test this hypothesis, we investigated whether the mutant TaxK88A, defective in CBP/p300 binding, could exert similar repressive effect on ISGF3-directed transcription. As shown in Fig. 4A, the inhibitory effect of Tax on IFN-α-stimulated luciferase expression from pISRE-luc was completely abrogated by the mutation introduced in TaxK88A, revealing a correlation between CBP/p300-binding and ISGF3 repression. Similar result was obtained from the reporter assay with pGAL4-Stat2(TA) and pGAL4-luc, confirming that the binding of Tax to CBP/p300 is responsible for the inhibition of STAT2 and ISGF3 transactivation by Tax. Comparable expression of Tax and TaxK88A in each transfectant was confirmed by Western blot analysis (Fig. 4B).

To further verify the hypothesis that competition for limiting CBP/p300 is a mechanism for the observed Tax-mediated ISGF3 inhibition, we

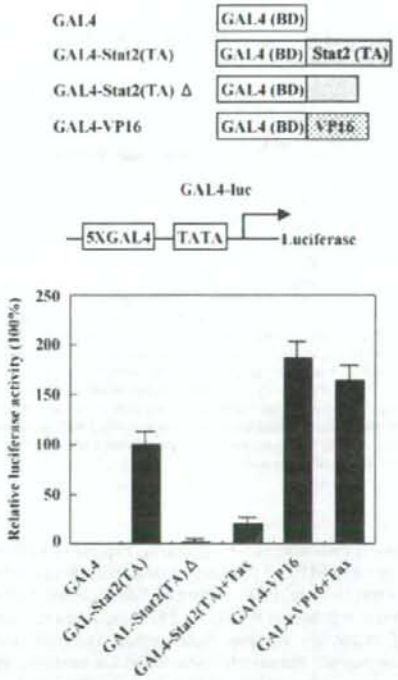

Fig. 3. Inhibition of STAT2 transactivation function by Tax. GAL4 carries the DNA binding domain only; GAL4-Stat2(TA) and GAL4-VP16 contain the transactivation domain of STAT2 and VP16 fused directly with the binding domain of GAL4; GAL4-Stat2(TA)Δ is a mutant of GAL4-Stat2(TA) with C-terminal 83 amino acids of STAT2 deleted. HeLa cells were transfected with the indicated expression constructs together with the GAL4-luc reporter vector, and luciferase activities were determined and calculated as described for Fig. 1. The results are from four independent triplicate experiments.

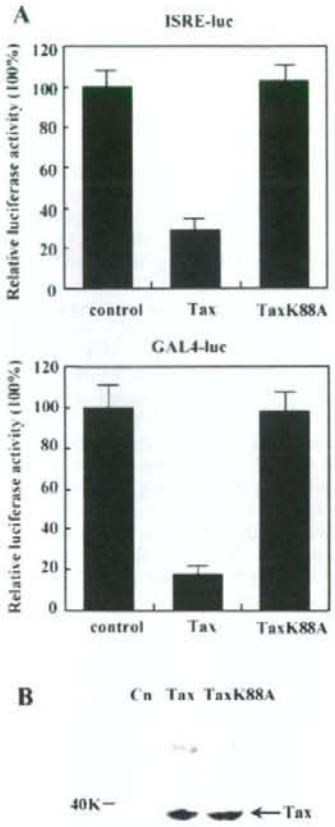

Fig. 4. Tax's ability to bind to CBP is critical for its repressive effect on STAT2 transactivation. (A) Huh-7 cells were transfected with ISRE-luc (upper) or GAL4-luc (lower) together with pCn, pCnwtax or pCnTaxK88A. Mutant TaxK88A harbors an amino acid substitution at condon 88 from lysine to alanine and is defective in CBP/p300 binding. Cells were treated with 100 IU/ml of human IFN-α 24 h later, and the luciferase activity was measured following a further incubation for 24 h. Renilla luciferase activities from cotransfected pRL-TK were used to normalize the transfection efficiency. Normalized luciferase activity from an otherwise identical control transfection with pCn vector was set as 100%, and those in other transfectants are expressed as relative percentage. Representative data are from five independent triplicate transfections. (B) Similar level of Tax expression in cells transfected with pCnwtax or pCnTaxK88A. Cells transfected with each indicated construct were harvested 48 h posttransfection, and Western blot analysis was performed using anti-Tax antibody (AS-5703). Solid arrow indicates the signals of Tax protein.

next investigated whether exogenously expressed CBP/p300 could restore the reduced ISGF3 transcriptional activity by Tax. In the absence of Tax, expression of p300 enhanced ISRE-directed luciferase gene expression in response to IFN-α (Fig. 5A), indicating a rate limiting level of p300 within the nucleus. Noteworthily, cotransfection of p300 expression plasmid completely restored the Tax-mediated inhibition of ISGF3 transactivation. Western blot analysis showed a similar Tax expression in Huh-7 cells irrespective of whether p300 was expressed or not (Fig. 5B), excluding the possibility that derepression of ISGF3 function by overexpression of p300 is due to reduced Tax expression in cells overexpressing p300. Together, these results strongly suggest that Tax-mediated inhibition of ISGF3 transactivation potential is mediated by competitive usage of CBP/p300 between Tax and STAT2.

Competition between Tax and STAT2 for p300 binding

To provide further evidence supporting the competition model proposed above, we next determined whether Tax could bind to p300 in competition with STAT2 in vitro. GST pull-down assay was performed using the GST-p300$^{302-661}$ fusion protein containing GST fused to amino acids 302–661 of p300, which encompasses the homologous region of the CH1 and KIX domains of CBP. Purified GST-p300$^{302-661}$ was bound to glutathione-agarose beads and then incubated with labeled in vitro translated Tax or STAT2 protein. Purified GST was included as a negative control. As expected, either Tax or STAT2 bound well to GST-p300$^{302-661}$ (Fig. 6, lanes 3–4), while no interaction was detected with GST alone (Fig. 6A, lanes 1–2). Notably, inclusion of increasing amount of purified Tax protein in the binding mixture dose-dependently reduced STAT2 binding to GST-p300$^{302-661}$ (Fig. 6A, lanes 5–7). This finding indicates that Tax competes with STAT2 for binding to p300. To exclude the possibility that Tax could interact directly with STAT2 and thereby prevent STAT2 from binding to p300, the binding mixture was subject to immunoprecipitation with anti-Tax antibody. STAT2 was not co-precipitated with anti-Tax antibody (Fig. 6B, upper), whereas association of p300 with Tax was detected under the same condition (Fig. 6B, lower), indicating that Tax did not directly interact with STAT2. Together, these data support a competition between Tax and STAT2 for p300 binding, which may account for the observed repression of STAT2 by Tax.

Tax-mediated inhibition of JAK-STAT signaling is specific for IFN-α

In addition to STAT2, STAT1 has also been shown to interact with CBP/p300, which plays a role in IFN-γ-induced signal transduction. To address whether Tax might affect IFN-γ signaling via competition with STAT1 for binding to CBP/p300, Tax-expressing plasmid was transfected into Jurkat T cells together with pGAS-luc, a reporter

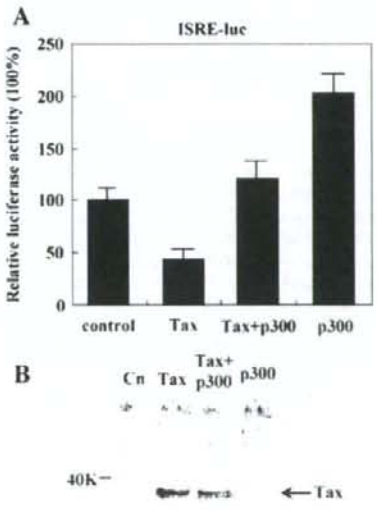

Fig. 5. Tax-mediated inhibition of STAT2 transactivation was reversed by overexpression of p300. (A) ISRE-luc reporter vector was transfected into Huh-7 cells together with pCn, pCnwtax and/or p300. Relative luciferase activities were determined and calculated as described for Fig. 1. Representative results are from three independent triplicate transfections. (B) Comparable Tax expression in cells irrespective of p300 co-expression was confirmed by Western blot analysis.

Fig. 6. (A) Tax inhibits STAT2 binding to p300. Labeled STAT2 or Tax in vitro translation product was incubated with GST alone (lanes 1–2) or GST-p300$^{302-661}$ (lanes 3–4). In competition assay (lanes 5–7), STAT2 was incubated with GST-p300$^{302-661}$ in the presence of increasing amount of Tax. (B) Tax does not directly interact with STAT2. The same reaction mixture was immunoprecipitated with anti-Tax antibody followed by Western blotting with anti-Stat2 (upper) or anti-p300 (lower) antibody.

vector encoding the luciferase gene under the control of tandem repeats of gamma-activated sequence (GAS) element that is recognized by STAT1 homodimer induced by IFN-γ. Cells were cultured in the absence or presence of 500 IU/ml of human IFN-γ 24 h later, and the luciferase activity was measured after an additional incubation for 24 h. As shown in Fig. 7A, the luciferase expression was significantly induced by treatment with IFN-γ, indicating the presence of functional IFN-γ receptor and STAT1 in Jurkat T cells. IFN-γ-induced luciferase expression was not significantly affected by cotransfection with either Tax- or TaxK88A-expressing plasmid. The luciferase expression under the control of HTLV-I LTR, which was monitored under the same condition, was substantially stimulated by cotransfection of Tax expression plasmid, suggesting that Tax was expressed and its function was intact in Jurkat T cells treated with IFN-γ (Fig. 7B). Further, expression of Tax was confirmed by immunoprecipitation and subsequent Western blot analysis with the antibody respectively recognizing the N and C terminus of Tax protein (data not shown). Together with the data shown in Fig. 1, it is suggested that Tax specifically modulates the JAK-STAT pathway in respond to IFN-α while having no effect on the signaling via IFN-γ.

Discussion

CBP/p300 regulates a variety of transcription factors involved in multiple signal transduction pathways, and competition between various classes of transcription factors for limiting amounts of CBP/p300 has been suggested as a repression mechanism to coordinate the transcriptional regulation of relevant genes. The transcriptional outcomes of simultaneous stimulation of two or more signal transduction pathways would depend on the abundance of the transcriptional factors and their relative affinities for CBP/p300. Inhibition of Ap1-dependent gene activation by steroid receptors and STAT1, for example, has been demonstrated to be attributable to competitive usage of CBP/p300 (Horvai et al., 1997; Kamei et al., 1996). Similarly, several oncogenic viruses encode viral proteins that bind to CBP/p300 and consequently deregulate CBP/p300-mediated transcription. HTLV-1-encoded Tax protein is among the best known of these. Indeed, multiple studies have linked Tax's binding to CBP/p300 with its repressive effect on the transcription directed by p53 (Ariumi et al., 2000), p73 (Ogryzko et al., 1996), c-Myb (Dai et al., 1996), and c-Jun (Van Orden et al., 1999), which also utilize CBP/p300 as the coactivator. Tax deregulation of the CBP/p300-mediated transcription, most of which are involved in apoptosis, cell cycle regulation, and differentiation, has significant implication in HTLV-1-associated malignant transformation.

Here, we investigated the effect of Tax protein on IFN-α-mediated signal pathway. Precedence for this study comes from our previous observation showing an attenuated IFN-α-induced antiviral response in Tax-expressing cells (Zhang et al., 2007), providing an explanation for the clinical study revealing a significantly lower rate of sustained IFN-α response in HCV/HTLV co-infected individuals, relative to those infected with HCV alone (Kishihara et al., 2001). The results presented here indicate that Tax interferes with IFN-α-induced JAK-STAT pathway, and the molecular basis for Tax-mediated IFN-α inhibition appears to be the competition between Tax and STAT2 for coactivator CBP/p300. We inferred this conclusion based on the following observations. Firstly, Tax's abilities to activate CREB-dependent pathway (Fig. 1A) and to bind CBP (Fig. 4A) are necessary for its repression on ISGF3-directed transcription. Secondly, in the presence of Tax, the formation of DNA-binding ISGF3 complex is unaffected (Fig. 2A) nevertheless being functionally compromised in directing ISRE-driven gene expression. Thirdly, Tax dose-dependently inhibits the binding of STAT2 to p300 in vitro (Fig. 6A), and there is no direct interaction between Tax and STAT2 in immunoprecipitation assay (Fig. 6B). Finally, Tax also inhibits the transcriptional activity of GAL4-Stat2(TA) containing the transactivation domain of STAT2 fused with GAL4 DNA-binding domain (Fig. 3), and Tax repression on ISGF3 was restored by

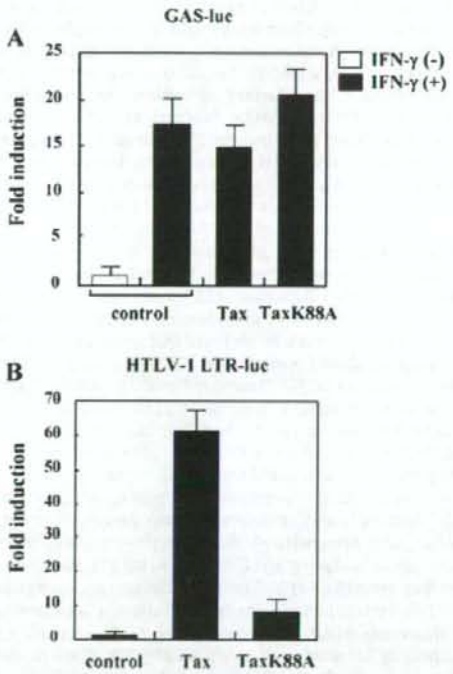

Fig. 7. Tax does not affect JAK-STAT pathway in response to IFN-γ signaling. Jurkat T cells were transfected with GAS-luc (A) or HTLV-I LTR-luc (B) along with pCn, pCnwtax or pCnTaxK88A. Relative luciferase activities were determined as described for Fig. 1. Fold induction means the luciferase activity relative to that co-transfected with the control vector pCn. The results are from three independent triplicate experiments.

overexpression of p300 (Fig. 5A). Together, these findings strongly suggest that Tax competitively binds to CBP/p300 and disables its function in ISGF3-directed transcription.

Tax m319, which corresponds to the previously characterized M47 Tax mutant (Smith and Greene 1990), contains two amino acid mutations (L319R and L320S) in the carboxy-terminal domain. While Harrod et al. (1998) identified the KID-like domain around amino acid residues 81–95 as the major CBP-binding domain of Tax, Bex et al. (1998) reported that M47 mutant is impaired in CBP binding, thus explaining its inability to activate CREB pathway. A compromised interpretation is that the KID-like domain in Tax is critical for the recruitment of CBP/p300 but additional contact(s) might also be required for interaction of Tax with CBP/p300. Alternatively, the carboxy-terminal domain might play a role in maintaining the overall structure and/or promoting the conformational change to render the KID-like domain accessible to CBP/p300. If this is the case, the mutations in Tax m319 might attenuate the ability of Tax to sequester CBP/p300, thereby failing to suppress ISRE-luc expression. Actually, a similar observation was previously reported by Ariumi et al. (2000), who demonstrated that the mutations in Tax m319 abrogated the ability of Tax to repress p53-directed transcription by competitive binding to CBP. Further studies are now in progress to clarify this issue.

Repression of STAT2 by Tax is reminiscent of the scenario described in adenovirus-encoded E1A protein, which has been demonstrated to repress STAT2 transactivation and IFN-α-induced transcription at least in part through competition for CBP/p300 (Bhattacharya et al., 1996). In addition to these two viruses, viral proteins encoded by other oncogenic viruses, such as large T antigen from SV40 (Eckner et al., 1996) and polyomavirus (Cho et al., 2001), E6 protein from human papillomavirus (Patel et al., 1999), and Tat protein from HIV-1 (Ott et al., 1999), also bind to CBP/p300 and deregulate CBP/p300-mediated cellular transcription, it is thus probable, but remains to be proven, that an analogous anti-IFN strategy might also be employed by these viruses. It is known that interaction of Tax with the KIX domain of CBP/p300 is crucial for Tax-mediated coactivator recruitment, although additional contacts may further strengthen the interaction and contribute to Tax's transcription function. In the case of STAT2, previous studies have identified the CH1 domain as the binding site (Bhattacharya et al., 1996). CH1 domain is located immediately amino-terminal to the KIX domain. It is thus possible that steric hindrance or conformational changes following binding of Tax to CBP/p300 might result in the diminishment of STAT2 binding by blocking access of STAT2 to its binding sites. Additionally, it was reported that the transcriptional repression between Tax and p73β, c-Myb, c-Jun pathway is reciprocal (Lemasson and Nyborg, 2001; Van Orden et al., 1999). In a reporter assay to investigate whether STAT2 similarly repress Tax function, however, we found that overexpression of STAT2 didn't obviously affect Tax-stimulated HTLV-1 transcription (data not shown), suggesting that STAT2 could not inhibit binding of Tax to CBP/p300 and affect its ability to function as a coactivator in conjunction with CREB transcription factor. The failure of STAT2 to displace Tax from CBP/p300 is probably due to a higher affinity of Tax than STAT2 for CBP/p300. Alternatively, KIX domain may remain accessible for Tax binding and STAT2 displacement after binding of STAT2 to CH1 domain. Actually, a similar observation was previously reported by Riou et al., who demonstrated that Tax represses MyoD-dependent transcription by inhibiting MyoD-binding to the KIX domain of p300, but not vice versa (Riou et al., 2000). On the contrary, co-transfection of STAT2-expressing plasmid significantly inhibited Tax stimulation of HIV-1 transcription (data not shown), which involves activation of NF-κB pathway by Tax. Binding of STAT2 to CBP/p300 affects its ability to function as a coactivator in NF-κB- but not in CREB-dependent transcription, which may not be surprising considering that STAT2 binds to CH1 domain distinct from Tax and CREB, whereas both STAT2 and RelA of NF-κB share a common binding site (CH1) on CBP/p300. Consistent with this observation, binding of STAT2 to p300 in competition with RelA was demonstrated as the mechanism by which IFN-α inhibited TNF-α stimulation of HIV gene expression via NF-κB (Hottiger et al., 1998).

The data presented here indicate that Tax specifically deregulated the JAK-STAT pathway in respond to IFN-α but having no effect on the signaling via IFN-γ, suggesting that Tax did not interfere with the recruitment of CBP by STAT1. This is probably attributable to the fact that STAT1 interacts with the CH3 domain of CBP/p300 (Zhang et al., 1996), a region is relatively far from the binding site of Tax (KIX domain), and the CH3 domain may remain accessible for STAT1 binding after binding of Tax to KIX domain. Also, an alternative explanation for the different effects of Tax on IFN-α and IFN-γ signaling might be due to the difference in affinity of STAT2 and STAT1 for CBP/p300 binding, relative to that of Tax.

The ability of Tax to inhibit ISGF3 transactivation has potential biological implications. Like IFN-γ, IFN-α also plays a critical role in cancer immunosurveillance and immunoediting (Dunn et al., 2005). Impaired IFN-α signaling might therefore result in a loss of both the normal control of proliferation and regulation of apoptosis, thereby increasing the malignant behavior (Matin et al., 2001; Picaud et al., 2002). Indeed, reduced IFN-α-responsiveness has been linked to malignancy in various cancer types. For example, it was reported that deficiency in ISGF3 activity, due to suppressed expression of one or more components of ISGF3 complex, was involved in the pathogenesis of squamous cell carcinoma of the skin (Clifford et al., 2002). Further, it was demonstrated that stable expression of dominant negative STAT2 suppressed IFN-α-induced growth inhibitory response in highly IFN-α-sensitive human cells (Clifford et al., 2003). It is thus conceivable that repression of ISGF3 transactivation by Tax could contribute to the HTLV-1-associated malignancy by conferring a growth and/or survival advantage. Consistent with this hypothesis, it was previously reported that HTLV-1-infected T cells evade the antiproliferative action of IFN-β while having normal level of IFNAR1 expression and STAT phosphorylation (Smith et al., 1999). Additionally, ISGF3-directed transcription is a crucial step in transducing IFN-α-mediated antiviral response. The data presented here suggest that Tax-mediated ISGF3 inhibition might lead to a global repression of antiviral defense gene expression, thereby rendering unhindered viral replication. In addition to facilitating the replication of HTLV-1 itself, the antagonistic effect of Tax on IFN might also modulate the replication of other co-existing viral pathogens, providing a possible mechanism for the severer clinical consequence of viral infectious disease and poorer IFN-α responsiveness in patients co-infected with HTLV-1 (Boschi-Pinto et al., 2000; Kishihara et al., 2001). However, one concern in interpreting the physiological relevance of the results obtained here is that the level of Tax expression in HTLV-1-infected patients may be lower than that in established cell lines used here. In view that the titrating study was not performed here, it thus cannot be ruled out that Tax-mediated anti-IFN effect might be milder in vivo than that observed here.

While the manuscript was being prepared, Feng and Ratner reported that HTLV-1 down-regulates IFN-α-stimulated JAK-STAT signaling by reducing phosphorylation of tyrosine kinase 2 and STAT2, and provided evidence suggesting that Gag or Pr may be responsible for HTLV-1-mediated IFN-α inhibition (Feng and Ratner, 2008). Our data, however, do not support that Tax perturbs the events involved in the formation of DNA-binding ISGF3 complex. As shown in the result of EMSA (Fig. 2A), IFN-α-induced ISGF3 formation in Huhwtax was similar to that detected in HuhCn cells. Huhwtax constitutively expresses Tax protein at a level comparable to that in HTLV-1-infected MT-2 cells (Fig. 2B), and moreover this level of Tax expression conferred an attenuated IFN-α-induced antiviral response in Huhwtax cells (Zhang et al., 2007). Thus, the possibility that unaffected formation of ISRE-binding ISGF3 complex in Huhwtax was due to insufficient Tax expression in these cells was largely lessened, if could not be ruled out completely, allowing us to infer that Tax inhibits IFN-α signaling via a mechanism other than derailing the events involved in the formation of DNA-binding ISGF3 complex.

Nonetheless, the data presented here are not contradictory to the conclusion drawn from the Ratner's study, and it is possible that different HTLV gene products may act at different level of the JAK-STAT signaling to counteract IFN's action. Actually, it is frequently that viruses employ more than one strategy to evade IFN system.

In conclusion, we investigated here the effect of HTLV-1-encoded Tax protein on IFN-α signaling pathway, and provide evidence demonstrating that Tax negatively modulates IFN-α-induced JAK-STAT pathway by competing with STAT2 for coactivator CBP/p300. Tax preventing IFN-α from inducing an antiviral state and programming cell death provides an additional mechanism for the role of Tax in persistent viral infection and development of ATLL in HTLV-1-infected individuals, highlighting the significance of the anti-HTLV strategies targeting Tax protein.

Materials and methods

Plasmids

Empty plasmid pCn, and plasmids encoding wild-type HTLV Tax (pCnwtax) or its mutants (pCnm148 and pCnm319, K88A) have all been described previously (Yamaoka et al; 1996; Zhang et al., 2007; Harrod et al., 1998). The reporter vectors, pISRE-luc and pGAS-luc, were purchased from Stratagene. For construction of pGAL4-Stat2(TA), the cDNA of STAT2 transactivation domain (amino acids 670–851) was amplified with primers 5′-atctgcgatcgccatgCGGGATGAAGCTTTT-GGGTG-3′ and 5′-acctgtttaaacCTAGAAGTCAGAAGGCAT-3′, digested with Sgf I and Pme I, and ligated into in pFN11A(BIND) Flexi vector (Promega), which had been cut with the same enzymes immediate downstream of GAL4 DNA-binding domain. The cDNA insert for pGEX-p300 (amino acids 302–661) was generated by PCR using primers 5′-ataggatccatgGGTCAACAGCCAGCCCCG-3′ and 5′-agagaattctcaAG-CATTTGGTAGCATGTTCTG-3′, digested with BamH I and EcoR I and ligated into BamH I/EcoR I-digested pGEX-2Z (Amersham). The sequences of these constructs were confirmed by nucleotide sequencing.

Cells

Human hepatoma cell line Huh-7 and human cervical carcinoma HeLa cells were purchased from the American Type Culture Collection (ATCC) and maintained in Dulbecco's modified Eagle's medium (DMEM, Invitrogen) supplemented with 10% fetal calf serum and 50 U/ml penicillin and streptomycin. Jurkat T-lymphocytes were maintained in RPMI1640 medium supplement with 15% fetal calf serum. The cell line Huhwtax, which stably expresses Tax at a level comparable to HTLV-1-infected MT-2 cells, was established by transfecting Huh-7 cells with pCnwtax followed by G418 selection and limiting dilution.

Transient transfection and luciferase assay

Cells were seeded at 1×10^5 in 1 ml medium per well of 12-well plates 24 h before transfection. Indicated plasmid DNAs were transfected into cells with FuGENE6 (Roche). For each transfection, pRL-TK (Promega) vector was cotransfected as an internal control to normalize the transfection efficiency. The cells were harvested at 48 h posttransfection, and the cell lysates were prepared for luciferase assays with Dual-Luciferase Reporter Assay System (Promega) according to the manufacturer's instruction. Luciferase activities were measured using a TD-20/20 Luminometer (Promega).

EMSA

The probe used in the EMSA was obtained by annealing biotinylated consensus ISRE oligonucleotides $(AGGAAATAGAAACTG)_2$ and its complement. Nuclear extracts were prepared from the cells treated with or without IFN-α using NE-PER Nuclear and Cytoplasmic Extraction Reagent Kit (Pierce). EMSA was performed with the Lightshift Chemiluminescent EMSA Kit (Pierce) and the signals were detected with streptavidin-horseradish peroxidase conjugate and chemiluminescent substrate. For competition experiments, unlabeled double-strand oligonucleotides were used in a 50-fold molar excess. For supershift experiments, nuclear extracts were pre-incubated for 30 min with specific antibodies before addition to the binding reaction.

GST pull-down assay

GST-$p300^{302-661}$ fusion protein was induced by isopropyl-thiogalactopyranoside in BL21 *Escherichia coli* transformed with pGEX-p300, purified by binding to glutathione-Sepharose 4B (Bulk GST Purification Module, GE Healthcare), and dialyzed with PBS overnight. Tax and STAT2 proteins were in vitro translated with the TNT-coupled reticulocyte lysate systems kit (Promega) and labeled with Transcend tRNA (Promega). GST or GST-$p300^{302-661}$ was incubated with Tax or STAT2 in binding buffer. GS4B beads were added and incubated for 1 h. Proteins that bound to the beads were separated by SDS/PAGE and detected with streptavidin-horseradish peroxidase and chemiluminescent substrate.

Western blot analysis

Separation of protein on sodium dodecyl sulfate-polyacrylamide gel electrophoresis followed standard methods. After the proteins were transferred to Hybond-P PVDV Membrane (GE Healthcare), the membranes were blocked and then probed with monoclonal antibody specific for HTLV-I Tax (AS-5703, Microbix Biosystems Inc.), and signals were visualized with ECL Plus Western Blotting Detection Reagents (GE Healthcare).

References

Ariumi, Y., Kaida, A., Lin, J.Y., Hirota, M., Masui, O., Yamaoka, S., Taya, Y., Shimotohno, K., 2000. HTLV-1 tax oncoprotein represses the p53-mediated trans-activation function through coactivator CBP sequestration. Oncogene 19 (12), 1491–1499.

Bannister, A.J., Kouzarides, T., 1996. The CBP co-activator is a histone acetyltransferase. Nature 384 (6610), 641–643.

Bex, F., Yin, M.J., Burny, A., Gaynor, R.B., 1998. Differential transcriptional activation by human T-cell leukemia virus type I Tax mutants is mediated by distinct interaction with CREB binding protein and p300. Mol. Cell. Biol. 18 (4), 2392–2405.

Bhattacharya, S., Eckner, R., Grossman, S., Oldread, E., Arany, Z., D'Andrea, A., Livingston, D.M., 1996. Cooperation of Stat2 and p300/CBP in signalling induced by interferon-alpha. Nature 383 (6598), 344–347.

Boschi-Pinto, C., Stuver, S., Okayama, A., Trichopoulos, D., Orav, E.J., Tsubouchi, H., Mueller, N., 2000. A follow-up study of morbidity and mortality associated with hepatitis C virus infection and its interaction with human T lymphotropic virus type I in Miyazaki, Japan. J. Infect. Dis. 181 (1), 35–41.

Cho, S., Tian, Y., Benjamin, T.L., 2001. Binding of p300/CBP co-activators by polyoma large T antigen. J. Biol. Chem. 276 (36), 33533–33539.

Chrivia, J.C., Kwok, R.P., Lamb, N., Hagiwara, M., Montminy, M.R., Goodman, R.H., 1993. Phosphorylated CREB binds specifically to the nuclear protein CBP. Nature 365 (6449), 855–859.

Clifford, J.L., Walch, E., Yang, X., Xu, X., Alberts, D.S., Clayman, G.L., El-Naggar, A.K., Lotan, R., Lippman, S.M., 2002. Suppression of type I interferon signaling proteins is an early event in squamous skin carcinogenesis. Clin. Cancer Res. 8 (7), 2067–2072.

Clifford, J.L., Yang, X., Walch, E., Wang, M., Lippman, S.M., 2003. Dominant negative signal transducer and activator of transcription 2 (STAT2) protein: stable expression blocks interferon alpha action in skin squamous cell carcinoma cells. 2003. Mol. Cancer Ther. 2 (5), 453–459.

Dai, P., Akimaru, H., Tanaka, Y., Hou, D.X., Yasukawa, T., Kanei-Ishii, C., Takahashi, T., Ishii, S., 1996. CBP as a transcriptional coactivator of c-Myb. Genes Dev. 10 (5), 528–540.

Dunn, G.P., Bruce, A.T., Sheehan, K.C., Shankaran, V., Uppaluri, R., Bui, J.D., Diamond, M.S., Koebel, C.M., Arthur, C., White, J.M., Schreiber, R.D., 2005. A critical function for type I interferons in cancer immunoediting. Nat. Immunol. 6 (7), 722–729.

Eckner, R., Ewen, M.E., Newsome, D., Gerdes, M., DeCaprio, J.A., Lawrence, J.B., Livingston, D.M., 1994. Molecular cloning and functional analysis of the adenovirus E1A-associated 300-kD protein (p300) reveals a protein with properties of a transcriptional adaptor. Genes Dev. 8 (8), 869–884.

Eckner, R., Ludlow, J.W., Lill, N.L., Oldread, E., Arany, Z., Modjtahedi, N., DeCaprio, J.A., Livingston, D.M., Morgan, J.A., 1996. Association of p300 and CBP with simian virus 40 large T antigen. Mol. Cell. Biol. 16 (7), 3454–3464.

Feng, X., Ratner, L., 2008. Human T-cell leukemia virus type 1 blunts signaling by interferon alpha. Virology 374 (1), 210–216.
Gessain, A., Barin, F., Vernant, J.C., Gout, O., Maurs, L., Calender, A., de The, G., 1985. Antibodies to human T-lymphotropic virus type-I in patients with tropical spastic paraparesis. Lancet 2 (8353), 407–410.
Giebler, H.A., Loring, J.E., van Orden, K., Colgin, M.A., Garrus, J.E., Escudero, K.W., Brauweiler, A., Nyborg, J.K., 1997. Anchoring of CREB binding protein to the human T-cell leukemia virus type 1 promoter: a molecular mechanism of Tax transactivation. Mol. Cell. Biol. 17 (9), 5156–5164.
Gill, P.S., Harrington Jr., W., Kaplan, M.H., Ribeiro, R.C., Bennett, J.M., Liebman, H.A., Bernstein-Singer, M., Espina, B.M., Cabral, L., Allen, S., Kornblau, S., Pike, M.C., Levine, A.M., 1995. Treatment of adult T-cell leukemia-lymphoma with a combination of interferon alfa and zidovudine. N. Engl. J. Med. 332 (26), 1744–1748.
Grassmann, R., Dengler, C., Müller-Fleckenstein, I., Fleckenstein, B., McGuire, K., Dokhelar, M.C., Sodroski, J.G., Haseltine, W.A., 1989. Transformation to continuous growth of primary human T lymphocytes by human T-cell leukemia virus type I X-region genes transduced by a Herpesvirus saimiri vector. Proc. Natl. Acad. Sci. U.S.A. 86 (9), 3551–3555.
Grassmann, R., Berchtold, S., Radant, I., Alt, M., Fleckenstein, B., Sodroski, J.G., Haseltine, W.A., Ramstedt, U., 1992. Role of human T-cell leukemia virus type 1 X region proteins in immortalization of primary human lymphocytes in culture. J. Virol. 66 (7), 4570–4575.
Harrod, R., Tang, Y., Nicot, C., Lu, H.S., Vassilev, A., Nakatani, Y., Giam, C.Z., 1998. An exposed KID-like domain in human T-cell lymphotropic virus type 1 Tax is responsible for the recruitment of coactivators CBP/p300. Mol. Cell. Biol. 18 (9), 5052–5061.
Hermine, O., Bouscary, D., Gessain, Turlure, P., Leblond, V., Franck, N., Buzyn-Veil, A., Rio, B., Macintyre, E., Dreyfus, F., Bazarbachi, A., 1995. Treatment of adult T-cell leukemia-lymphoma with zidovudine and interferon alfa. N. Engl. J. Med. 332 (26), 1749–1751.
Horvai, A.E., Xu, L., Korzus, E., Brard, G., Kalafus, D., Mullen, T.M., Rose, D.W., Rosenfeld, M.G., Glass, C.K., 1997. Nuclear integration of JAK/STAT and Ras/AP-1 signaling by CBP and p300. Proc. Natl. Acad. Sci. U.S.A. 94 (4), 1074–1079.
Hottiger, M.O., Felzien, L.K., Nabel, G.J., 1998. Modulation of cytokine-induced HIV gene expression by competitive binding of transcription factors to the coactivator p300. EMBO J. 17 (11), 3124–3134.
Janknecht, R., Hunter, T., 1996. Transcription. A growing coactivator network. Nature 383 (6595), 22–23.
Kamei, Y., Xu, L., Heinzel, T., Torchia, J., Kurokawa, R., Gloss, B., Lin, S.C., Heyman, R.A., Rose, D.W., Glass, C.K., Rosenfeld, M.G., 1996. A CBP integrator complex mediates transcriptional activation and AP-1 inhibition by nuclear receptors. Cell 85 (3), 403–414.
Kishihara, Y., Furusyo, N., Kashiwagi, K., Mitsutake, A., Kashiwagi, S., Hayashi, J., 2001. Human T lymphotropic virus type 1 infection influences hepatitis C virus clearance. J. Infect. Dis. 184 (9), 1114–1119.
Kwok, R.P., Laurance, M.E., Lundblad, J.R., Goldman, P.S., Shih, H., Connor, L.M., Marriott, S.J., Goodman, R.H., 1996. Control of cAMP-regulated enhancers by the viral transactivator Tax through CREB and the co-activator CBP. Nature 380 (6575), 642–646.
Lemasson, I., Nyborg, J.K., 2001. Human T-cell leukemia virus type I tax repression of p73beta is mediated through competition for the C/H1 domain of CBP. J. Biol. Chem. 276 (19), 15720–15727.
Matin, S.F., Rackley, R.R., Sadhukhan, P.C., Kim, M.S., Novick, A.C., Bandyopadhyay, S.K., 2001. Impaired alpha-interferon signaling in transitional cell carcinoma: lack of p48 expression in 5637 cells. Cancer Res. 61 (5), 2261–2266.
Ogryzko, V.V., Schiltz, R.L., Russanova, V., Howard, B.H., Nakatani, Y., 1996. The transcriptional coactivators p300 and CBP are histone acetyltransferases. Cell 87 (5), 953–959.
Osame, M., Usuku, K., Izumo, S., Ijichi, N., Amitani, H., Igata, A., 1986. HTLV-I associated myelopathy, a new clinical entity. Lancet 1 (8488), 1031–1032.
Ott, M., Schnölzer, M., Garnica, J., Fischle, W., Emiliani, S., Rackwitz, H.R., Verding, E., 1999. Acetylation of the HIV-1 Tat protein by p300 is important for its transcriptional activity. Curr. Biol. 9 (24), 1489–1492.
Patel, D., Huang, S.M., Baglia, L.A., McCance, D.J., 1999. The E6 protein of human papillomavirus type 16 binds to and inhibits co-activation by CBP and p300. EMBO J. 18 (18), 5061–5072.
Picaud, S., Bardot, B., De Maeyer, E., Seif, I., 2002. Enhanced tumor development in mice lacking a functional type I interferon receptor. J. Interferon Cytokine Res. 22 (4), 457–462.
Riou, P., Bex, F., Gazzolo, L., 2000. The human T cell leukemia/lymphotropic virus type 1 Tax protein represses MyoD-dependent transcription by inhibiting MyoD-binding to the KIX domain of p300. A potential mechanism for Tax-mediated repression of the transcriptional activity of basic helix-loop-helix factors. J. Biol. Chem. 275 (14), 10551–10560.
Smith, D., Buckle, G.J., Hafler, D.A., Frank, D.A., Hollsberg, P., 1999. HTLV-I-infected T cells evade the antiproliferative action of IFN-beta. Virology 257 (2), 314–321.
Smith, M.R., Greene, W.C., 1990. Identification of HTLV-I tax trans-activator mutants exhibiting novel transcriptional phenotypes. Genes Dev. 4 (11), 1875–1885.
Sun, W.H., Pabon, C., Alsayed, Y., Huang, P.P., Jandeska, S., Uddin, S., Platanias, L.C., Rosen, S.T., 1998. Interferon-alpha resistance in a cutaneous T-cell lymphoma cell line is associated with lack of STAT1 expression. Blood 91 (2), 570–576.
Van Orden, K., Giebler, H.A., Lemasson, I., Gonzales, M., Nyborg, J.K., 1999. Binding of p53 to the KIX domain of CREB binding protein. A potential link to human T-cell leukemia virus, type I-associated leukemogenesis. J. Biol. Chem. 274 (37), 26321–26328.
Yamaoka, S., Inoue, H., Sakurai, M., Sugiyama, T., Hazama, M., Yamada, T., Hatanaka, M., 1996. Constitutive activation of NF-kB is essential for transformation of rat fibroblasts by the human T-cell leukemia virus type I Tax protein. EMBO J. 15 (4), 873–887.
Yang, X.J., Ogryzko, V.V., Nishikawa, J., Howard, B.H., Nakatani, Y., 1996. A p300/CBP-associated factor that competes with the adenoviral oncoprotein E1A. Nature 382 (6589), 319–324.
Yoshida, M., Seiki, M., Yamaguchi, K., Takatsuki, K., 1984. Monoclonal integration of human T-cell leukemia provirus in all primary tumors of adult T-cell leukemia suggests causative role of human T-cell leukemia virus in the disease. Proc. Natl. Acad. Sci. U.S.A. 81 (19), 2534–2537.
Zhang, J.J., Vinkemeier, U., Gu, W., Chakravarti, D., Horvath, C.M., Darnell Jr., J.E., 1996. Two contact regions between Stat1 and CBP/p300 in interferon gamma signaling. Proc. Natl. Acad. Sci. U.S.A. 93 (26), 15092–15096.
Zhang, J., Yamada, O., Kawagishi, K., Yoshida, H., Araki, H., Yamaoka, S., Hattori, T., Shimotohno, K., 2007. Up-regulation of hepatitis C virus replication by human T cell leukemia virus type I-encoded Tax protein. Virology 369 (1), 198–205.

Characterization of a CD4-independent clinical HIV-1 that can efficiently infect human hepatocytes through chemokine (C-X-C motif) receptor 4

Peng Xiao[a,b], Osamu Usami[a], Yasuhiro Suzuki[a], Hong Ling[b], Nobuaki Shimizu[c], Hiroo Hoshino[c], Min Zhuang[b], Yugo Ashino[a], Hongxi Gu[b] and Toshio Hattori[a]

Objective: HIV-1 isolates are prominently CD4-dependent and, to date, only a few laboratory-adapted CD4-independent strains have been reported. Therefore, whether CD4-independent viruses may exist in HIV-1-infected patients has remained unclear. Here, we report the successful isolation of a CD4-independent clinical HIV-1 strain, designated SDA-1, from the viral quasispecies of a therapy-naive HIV-1 and *Pneumocystis jirovecii* pneumonia patient in the late-stage of AIDS with extremely low CD4 cell count (CD4 = 1/μl). We characterized this virus and further explored whether it could infect or induce pathological effects in human hepatocytes.

Design and methods: To determine coreceptor usage and CD4-independent infection, the HIV-1 envelope (Env)-pseudotypes and Env-chimeric viruses were used.

Results: SDA-1 was able to infect $CD4^-$ cell lines through either chemokine (C-X-C motif) receptor 4 or CCR5. It still maintained the ability to infect $CD4^+$ cells through multiple coreceptors of chemokine (C-X-C motif) receptor 4, chemokine (C-C motif) receptor 5, chemokine (C-C motif) receptor 3 and chemokine (C-C motif) receptor 8. Productive infection by SDA-1 was noted in both CD4-negative hepatoma cells and primary cultured human hepatocytes. Moreover, we demonstrated that SDA-1 could efficiently infect human hepatocytes on both static and mitotic phases through chemokine (C-X-C motif) receptor 4, without inducing apoptotic cell death.

Conclusion: The present study provides evidence that emergence of CD4-independent HIV-1 virus *in vivo* may occur in HIV-1-infected patients. In addition, these results shed light on the mechanisms involved in liver damage in HIV-1-infected individuals, which could have important implications concerning the range of mutability and the pathogenesis of AIDS.

AIDS 2008, **22**:1749–1757

Keywords: CD4-independence, HIV-1, human hepatocytes, human hepatoma cells

Introduction

The entry of HIV-1 into target cells requires interaction of the viral envelope (Env) with CD4 and a chemokine coreceptor [1,2]. Macrophage-tropic HIV-1 viruses primarily use chemokine (C-C motif) receptor 5 (CCR5) (R5) as a coreceptor, whereas T-cell-tropic viruses use chemokine (C-X-C motif) receptor 4

[a]Department of Emerging Infectious Diseases, Division of Internal Medicine, Graduate School of Medicine, Tohoku University, Sendai, Japan, [b]Department of Microbiology, Harbin Medical University, Harbin, China, and [c]Department of Virology and Preventive Medicine, Gunma University School of Medicine, Gunma, Japan.

Correspondence to Toshio Hattori, MD, PhD, Department of Emerging Infectious Diseases, Division of Internal Medicine, Graduate School of Medicine, Tohoku University, Sendai 980-8574, Japan.

Tel: +81 22 717 8220; fax: +81 22 717 8221; e-mail: hattori.t@rid.med.tohoku.ac.jp
Received: 17 January 2008; revised: 21 April 2008; accepted: 9 May 2008.

DOI:10.1097/QAD.0b013e328308937c

ISSN 0269-9370 © 2008 Wolters Kluwer Health | Lippincott Williams & Wilkins

(CXCR4) (X4). Dual-tropic viruses (R5X4) use both coreceptors [3]. A few rare viruses can also use alternative coreceptors such as chemokine (C-C motif) receptor 1 (CCR1), chemokine (C-C motif) receptor 2b (CCR2b), chemokine (C-C motif) receptor 8 (CCR8), chemokine (C-X-C motif) receptor 6 (CXCR6), G protein-coupled receptor 1 (GPR1) or GPR15/Bob for entry into coreceptor-transfected $CD4^+$ cell lines [4]. Whatever the coreceptor specificity of an HIV-1 isolate, an interaction with CD4 is always the first step in a chain of events leading to fusion of the viral envelope with the cellular membrane. However, previous studies have shown that SIV [5] and HIV-2 [6] can also infect cells independently of CD4.

In contrast to SIV and HIV-2, HIV-1 CD4-independent viruses are rarely isolated. To date, only a few laboratory CD4-independent HIV-1 variants [7–10] have been reported. Therefore, whether such viruses may exist in HIV-1-infected patients has remained unclear. However, several studies [11–14] have shown that HIV-1-DNA and p24, a core HIV-1 antigen, were detected in CD4-negative cells or tissues such as brain, kidney and liver in HIV-infected individuals, suggesting the possibility that low levels of CD4-independent variants exist *in vivo*. Among such $CD4^-$ cells or tissues, liver is an important organ in determining the prognosis of HIV-1-infected patients. End-stage liver disease is becoming a frequent cause of death in HIV-1-infected hospitalized patients [15–17]. Although the cause of liver injury in HIV-1 patients might be multifactorial, such as hepatitis B virus (HCV) and hepatitis B virus (HBV) coinfection and the side effects of antiretroviral therapy, a number of reports have documented that histological liver abnormalities occurred solely as a result of HIV-1 infection [13,18,19]. Nonetheless, few attempts have been made to elucidate the mechanisms of the liver damage in HIV-1-infected individuals.

In this study, we successfully isolated a CD4-independent clinical HIV-1 strain, designated SDA-1, from the viral quasispecies of a therapy-naive HIV-1 and *Pneumocystis jirovecii* pneumonia (PJP) patient in the late stage of AIDS with extremely low CD4 cell numbers. We characterized the phenotype of this virus and further explored whether it could infect or induce pathological effects in human hepatocytes.

Materials and methods

Patient's information

A 53-year-old Japanese man infected with HIV-1 was admitted to Tohoku University Hospital owing to prolonged fever and severe dyspnea in 2000. His plasma viral load and CD4 cell count at the time of admission was 220 000 copies/ml and 1 cell/μl, respectively. He was diagnosed with PJP, and his clinical stage was classified as IV-C3 [20]. The onset and route of HIV-1 infection were unknown. No evidence of coinfection with HBV or HCV in this patient was found. The patient was treated with trimethoprim and sulfamethoxazole (TMP–SMX) and highly active antiretroviral therapy (HAART). His condition deteriorated rapidly and he died 33 days after admission. Consent for autopsy was denied by the patient's family.

Before HAART, plasma samples and peripheral blood mononuclear cells (PBMC) were collected from this patient and cryopreserved in liquid nitrogen until use. The institutional Ethics Committee approved this study and written informed consent was obtained from the patient.

Virus isolation

HIV-1 isolation was achieved by using an in-vitro short-term phytohemagglutinin (PHA)–PBMC coculture method. Briefly, cryopreserved PBMC (2×10^6) from the patient were cocultivated with PHA-stimulated PBMC (5×10^6) from an HIV-1 seronegative healthy donor. The culture was maintained in RPMI-1640 (Invitrogen, California, USA) containing 10% fetal calf serum and 5 U/ml of recombinant interleukin-2 (IL-2) (Sigma, St. Louis, Missouri, USA). Proliferation of HIV-1 was examined by measuring p24 antigen in the cell culture supernatant using a p24 ELISA kit (RETRO-TEK, ZeptoMetrix Corp., New York, USA). The virus stocks were kept at −80 °C until use.

Amplification of *env* and sequence analysis

The full-length HIV-1 *env* genes were amplified by limiting dilution nested PCR from proviral PBMC DNA or plasma RNA as previously described [21,22]. To avoid artificial recombination and resampling of the viral genomes, independent nested PCR reactions were carried out per specimen [23,24].

The first round PCR was conducted with a F5852–R8935 primer pair (F5852, 5′-TAGAGCCCTGGAAG CATCCAGGAAG, HIV-1 HXB2 nucleotide position 5852–5876; R8935, 5′-TTGCTACTTGTGATTGCT CCATGT, HXB2 nucleotide position 8912–8935). The second round PCR was performed with a F5957–R8903 primer pair (F5957, 5′-GATCGAATTCTAGGCATC TCCTATGGCAGGAAGAAG, HXB2 nucleotide position 5957–5982, containing an additional *Eco*RI site (underlined) to facilitate cloning; R8903, 5′-AGCT CTC GAGGTCTCGAGATACTGCTCCCACCC, HXB2 nucleotide position 8881–8903, containing an additional *Xho*I site (underlined)). The purified PCR products were subcloned into the *Eco*RI and *Xho*I sites of the pSM-HXB2 plasmid. All correctly oriented *env* clones were then screened for biological function [22] followed by sequencing and phylogenetic analysis as previously described [25,26].

Cell lines and cell culture

All the cell lines, unless otherwise specifically mentioned, were cultured in Dulbecco's modified Eagle's medium (DMEM, Invitrogen) containing 10% fetal calf serum. Human glioma NP-2-CD4$^+$ cells transfected with a variety of chemokine receptors as indicated [27] were maintained in medium containing 500 μg/ml of G-418 (Promega, Wisconsin, USA) and 1 μg/ml of puromycin (Sigma). Human CD4-negative osteosarcoma (HOS) cells expressing either CXCR4 or CCR5 [28] were cultured in medium containing 1 μg/ml of puromycin. Human hepatoma cells Huh-7 and Hep-G2 [29] were obtained through the Cell Resource Center for Biomedical Research, Tohoku University, Japan. Human primary cultured hepatocytes (p-hepatocytes, BD Bioscience, California, USA) were maintained on BD Matrigel with Hepato-STIM hepatocyte culture medium (BD Bioscience).

Reagents and antibodies

The CXCR4 antagonist AMD3100 [30], and the CCR5 antagonist TAK-779 [31] were provided by the NIH AIDS Research and Reference Reagent Programme and Takeda Chemical Industries, Ltd., Osaka, Japan, respectively. Recombinant human soluble CD4 (sCD4) was from ImmunoDiagnostics, Inc. (Woburn, Massachusetts, USA). Antialbumin-fluorescein isothiocyanate (FITC) antibody was from Cedarlane Laboratories Ltd. (Hornby, Ontario, Canada). Anticytokeratin-18–phycoerythrin and antialpha fetoprotein (AFP)–FITC antibodies were from Santa Cruz Biotechnology, Inc. (Santa Cruz, California, USA). Anti-HIV-1-p24 (clone KC57)-FITC antibody was from Beckman Coulter. All other antibodies were from BD Pharmingen (San Diego, California, USA).

Pseudotyped virus infection assay

The HIV-1 Env-pseudotypes were generated as previously described [32]. Briefly, 293T cells (5×10^6 cells/10 cm-dish) were transfected with 5 μg of luciferase-expressing pNL4-3-Luc-R$^-$E$^-$ [33] or green fluorescent protein (GFP)-expressing pNL4-3-GFP [34] plasmid in combination with 10 μg of one of the *env*-expressing plasmids, pSM-SDA-1, pSM-HXB2 (X4), pSM-ADA (R5), or pSM-89.6 (R5X4). The vesicular stomatitis virus-G pseudotypes were also prepared [35].

For infection assays of luciferase-pseudotypes (luc-p), 10 ng p24 of luc-p were added into each well of 24-well plates (5×10^4 cells/well). After 12 h infection, the cells were washed and incubated for an additional 36 h at 37 °C. The cells were then lysed using a Luciferase Assay kit (Promega) and the luciferase activity was examined by a luminometer (Lumat 9507, Germany). To determine the effects of various reagents related to the viral receptors, target cells were preexposed for 1 h with the indicated concentration of the antagonists, or the antibodies. For GFP-pseudotypes (GFP-p) infection, target cells were infected with 10 ng p24 of GFP-p virus for 48 h and fixed by 5% paraformaldehyde. Infectivities were visualized under a Zeiss LSM510 confocal microscopy and DIC images with a 512 × 512 resolution were acquired.

Chimeric viruses

All *env* recombinant chimeric viruses in this study were generated in the background of pNL43, an X4-tropic HIV-1 infectious clone [36]. Briefly, the fragment of pNL43 containing *Eco*RI (nt 5743–5748) and *Kpn*I (nt 6343–6348) was amplified by PCR with a F5671–R6472 primer pair (F5671, 5′-GGCTCCATAACTTAGGA CAAC, pNL43 nucleotide position 5671–5691; R6472, 5′-TACTTCTTGTGGGTTGGGGTC, pNL43 position 6452–6472), followed by insertion into the pSM–SDA-1 using *Eco*RI and *Kpn*I. The new *Eco*RI–*Xho*I fragment (3155 bp) covering the entire SDA-1 *env* gene was then replaced with the equivalent region of pNL43 to construct the Env-chimeric virus NL43_SDA-1. Similarly, Env-chimeras of ADA (NL43_ADA), 89.6 (NL43_89.6) or truncated *env* (NL43_env (-)) were created, respectively. All Env-chimeric viruses were prepared by transfecting 293T cells as described above. For infection assays, 100 ng p24 of the chimeric viruses or virus stock supernatants were added in each well of 24-well plates (5×10^4 cells/well). After 2 h adsorption, the cells were washed and incubated for 48 h. Viral replication was monitored by p24 antigen production.

Flow cytometry and apoptosis assay

We performed cell-surface staining for CD4, CXCR4 and CCR5 by flow cytometry. To determine the purification and differentiation of p-hepatocytes, we tested the specific markers using antialbumin–FITC, anti-AFP–FITC and anticytokeratin-18–phycoerythrin antibodies. Appropriate class matched antibodies were used in each experiment. To detect the proliferation and intracellular p24, p-hepatocytes were fixed and permeabilized using a Cytofix-Cytoperm kit (BD Bioscience). Subsequently, the cells were stained with anti-Ki-67–phycoerythrin and antip24–FITC antibodies. Apoptosis of the p-hepatocytes was determined using the Apoptosis Detection kit I (BD Pharmingen). Flow cytometry analysis was performed using FACSCalibur (Becton Dickinson, New Jersey, USA). All Data were acquired and analyzed using Cell Quest software (BD Bioscience).

Nucleotide sequence accession number

The GenBank accession number for the sequence determined in this study is AY902478 (SDA-1).

Results

Evaluation of SDA-1 viral quasispecies

In an attempt to isolate CD4-independent clinical HIV-1 strain(s), we performed virus isolation from a

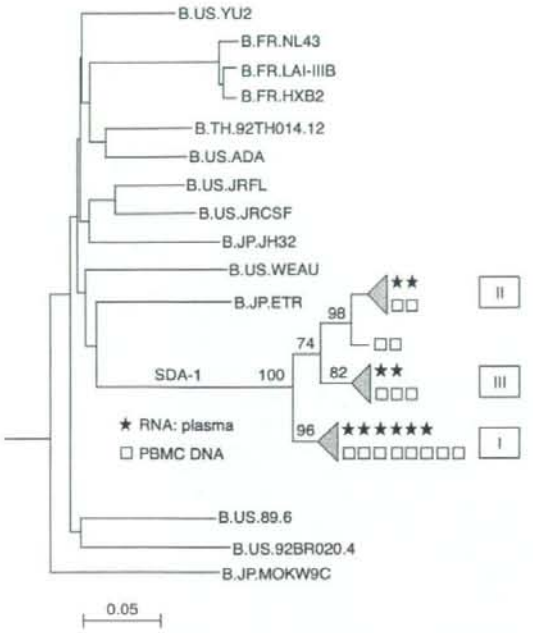

Fig. 1. Evolution of SDA-1 *env* quasispecies in plasma and PBMC. Phylogenetic analysis of newly characterized, SDA-1 gp120 *env* nucleotide sequences obtained from plasma ($n=10$) and PBMC ($n=15$) with representative sequences of HIV-1 subtype B. Numbers at branch nodes refer to the percentage of bootstrap values and symbols indicate individual clones.

therapy-naive HIV-1 and PJP patient with extremely low CD4 cell number, and successfully isolated the virus (peak of p24, 500 ng) from this patient and designated it SDA-1. To assess the quasispecies diversity present in *vivo*, we analyzed the SDA-1 *env* clones derived from plasma RNA and PBMC. As shown in Fig. 1, SDA-1 is grouped within the HIV-1 subtype B reference sequences. Within SDA-1's sequence cluster, three phylogenetic forms were identified. Supported by a significant bootstrap value (96%), form I was the predominant quasispecies, representing 70% of all sequences. Two minor quasispecies (forms II and III) had similar structures but differed in the position of the first breakpoint. The mean distances between major and minor quasispecies did not differ significantly from the sequence heterogeneity. Furthermore, the quasispecies diversities between plasma and PBMC were similar within each form, and were all below 5.0%.

Multicoreceptor usage and CD4-independent entry of SDA-1

To determine the receptor usage of SDA-1, we randomly selected five clones from the predominant quasispecies and generated Env-pseudotypes and Env-chimeric viruses as representatives. As a control, the Envs from a variety of HIV-1 subtypes with X4 (HXB2), R5 (ADA), and R5X4 (89.6) tropism were used. Utilizing luciferase-pseudotypes (luc-p), we first examined the coreceptor usage of SDA-1. We found that in the presence of CD4, all representative SDA-1 Env-pseudotypes were able to use efficiently both CXCR4 and CCR5, with additional moderate usage of CCR3 and CCR8 (Fig. 2a).

We next investigated whether SDA-1 Envs are capable of inducing CD4-independent infection. We found that SDA-1 Envs mediated entry into both HOS–CXCR4 and HOS–CCR5. However, the infectivities of SDA-1 for HOS–CXCR4 were approximately 2.5-fold higher than that for HOS–CCR5 (Fig. 2b). In stark contrast, none of the other types of luc-p viruses entered either of those cells. Furthermore, we evaluated the ability of SDA-1 Envs in mediating cell–cell fusion, a dye-transfer cell–cell fusion assay [37] was used with HOS–CXCR4 and HOS–CCR5 cells. Only in the cells expressing SDA-1 Envs (effector cells) did cell–cell fusion with CD4-negative, CXCR4- or CCR5-positive HOS cells (target cells) occur (data not shown).

In addition to the results with HOS–CXCR4 and CCR5, preexposure of HOS cells to Leu-3A, a CD4 monoclonal antibody (mAb) that recognizes the gp120 binding site on CD4 [38], failed to block SDA-1 infection. In contrast, pretreatment with antagonists for CXCR4 or CCR5 effectively inhibited infection (Table 1). Furthermore, the infectivities of SDA-1 on HOS–CXCR4 and HOS–CCR5 were enhanced by preexposure of the virus to sCD4 indicating that the binding of SDA-1 Env to CD4 induces further conformational changes in gp120 to fully expose the chemokine receptor binding domain. Collectively, SDA-1 Envs mediated the CD4-independent infection via both CXCR4 and CCR5.

Having clarified that SDA-1 is a CD4-independent isolate, we next investigated what types of $CD4^-$ cells are able to support SDA-1's entry. We focused first on human liver-derived cell lines, as the mechanisms of the liver damage in HIV-1-infected individuals are still unclear.

Two hepatoma cell lines, Huh-7 and Hep-G2, were used as targets. We first examined the expression of the receptors on the cell surface by flow cytometry and found that both CXCR4 and CCR5 were expressed on Huh-7 and Hep-G2 cells. In contrast, CD4 was not detected on either, which was confirmed by RT–PCR (data not shown). We then evaluated whether SDA-1 can enter into hepatoma cells with luc-p viruses. We found that only SDA-1 luc-p viruses efficiently infected Huh-7; however, its infectivity was marginal in Hep-G2 (Fig. 2c). Previous studies have shown that few HIV-1 variants can infect $CD8^+$ cells using CD8 as receptor [10,39]. Therefore, we further explored receptors used by

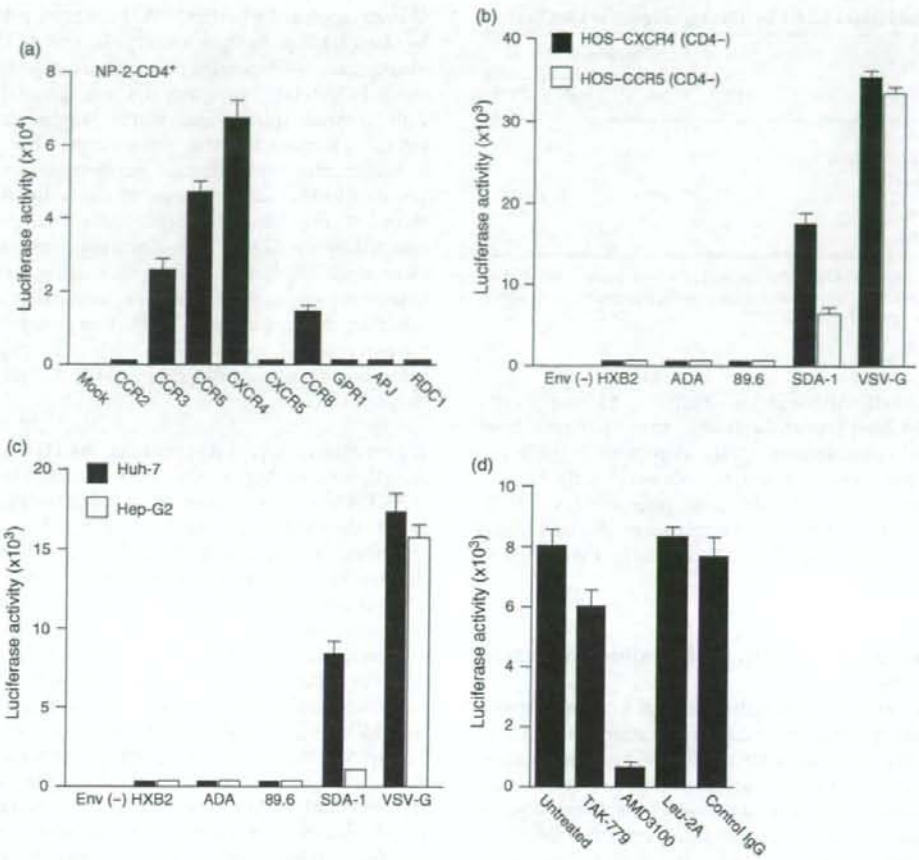

Fig. 2. Multicoreceptor usage and CD4-independent entry of SDA-1. (a) SDA-1 Envs mediate entry of $CD4^+$ cells using multiple coreceptors. NP-2-$CD4^+$ cells coexpressing one of the indicated chemokine receptors were exposed to SDA-1 luc-p viruses for 48 h and the luciferase activities were measured. (b) SDA-1 Envs mediate entry of $CD4^-$ cell lines through either CXCR4 or CCR5. The HOS cells ($CD4^-$) expressing either CXCR4 or CCR5 were exposed to the indicated HIV-1 luc-p viruses or VSV-G for 48 h, after which the infectivities were determined. (c) Entry of SDA-1 into $CD4^-$ human hepatoma cells. Huh-7 and Hep-G2 were exposed to the indicated HIV-1 luc-p viruses or VSV-G. Infectivities were determined at 48 h. (d) Effects of receptor-related antagonists or antibodies on the entry of SDA-1 entry into Huh-7 cells. Interaction of SDA-1 luc-p viruses with Huh-7 cells was tested in the absence or presence of AMD3100 (1.0 μM), TAK-779 (100 nM), anti-CD8 Leu-2A antibody (30 μg/ml) or class-matched control antibody (30 μg/ml). Results shown (a–d) are means of triplicate experiments. Bars, standard deviation. IgG, immunoglobulin G; VSV, vesicular stomatitis virus.

SDA-1 for entry into hepatoma cells. As shown in Fig. 2d, preexposure of Huh-7 to anti-CD8 Leu-2A mAb, as well as the CCR5 antagonist, TAK-779, failed to block SDA-1 infection of Huh-7, whereas anti-CXCR4 with AMD3100 effectively suppressed the infectivity. These results suggested that SDA-1 enters Huh-7 cells principally via CXCR4.

Replication of SDA-1 in human hepatoma cells

Although SDA-1 luc-p viruses infected some cells independently of CD4 cells, it was necessary to determine whether SDA-1 can replicate in those $CD4^-$ cells, particularly in hepatoma cells. For this purpose, we constructed NL43-based Env-chimeric viruses described above. We then examined whether the chimeric viruses were able to replicate in $CD4^-$ cells. As shown in Fig. 3a, the SDA-1 Env-chimeric viruses replicated efficiently in HOS–CXCR4 and HOS–CCR5 cells to similar levels. In contrast, none of the other Env-chimeric viruses infected either of those cells lines. Furthermore, we examined whether SDA-1 Env-chimeric viruses could replicate in hepatoma cells. As shown in Fig. 3b, high levels of NL43-SDA-1 replication were observed in Huh-7 cells. However, marginal replication was detected

Table 1. Inhibition of SDA-1 by blocking reagents in CD4⁻ cells.

Reagent	% Inhibition	
	HOS–CXCR4	HOS–CCR5
Medium	0	0
Control mAb (30 μg/ml)	0	0
Leu-3A (30 μg/ml)	10	12
Soluble CD4 (10 μg/ml)	225[a]	120[a]
AMD3100 (1.0 μM)	99	0
TAK-779 (100 nM)	0	97

CCR5, chemokine (C-C motif) receptor 5; CXCR4, chemokine (C-X-C motif) receptor 4; HOS, Human CD4-negative osteosarcoma; mAb, monoclonal antibody.
[a]Enhancement of entry.

in Hep-G2 cells. Although both Huh-7 and Hep-G2 cells are derived from human hepatoma, many potential host factors [40] could influence HIV replication, which for the most part remain unknown. Similarly, only Huh-7 cells, but not Hep-G2 cells, were susceptible to HCV [41,42]. These reasons may be related to the difference between Huh-7 and Hep-G2 regarding the level of replication by SDA-1.

SDA-1 replicates in both proliferating and static hepatocytes

To investigate further whether normal human hepatocytes could sustain entry and replication of SDA-1, p-hepatocytes were used for the following experiments. Among the three specific markers of human hepatocytes, both albumin and cytokeratin-18, but not alpha-fetoprotein were detected in the p-hepatocytes suggesting that the hepatocytes we used were well differentiated (data not shown). We also found that CXCR4 was expressed on the surface of p-hepatocytes. In contrast, neither CD4 nor CCR5 was detected on the p-hepatocyte surface or by real-time PCR (RT–PCR) (data not shown).

We next explored whether SDA-1 can enter p-hepatocytes by using GFP-p. As shown in Fig. 4a, only SDA-1 GFP-p viruses gave GFP-positive cells in p-hepatocytes, whereas other HIV-1 GFP-p viruses did not. The GFP-positive cells showed spindle-like shapes suggesting that the infection occurred in the p-hepatocytes but not in the contaminating lymphocytes. Furthermore, we studied whether SDA-1 can replicate in the p-hepatocytes. As shown in Fig. 4b, the p-hepatocytes were productively infected by the SDA-1 Env-chimeric viruses and SDA-1 virus stock itself but not by the other HIV-1 Env-chimeric viruses. Moreover, we found that AMD3100 inhibited the replication of SDA-1 in p-hepatocytes in a dose-dependent manner (Fig. 4c) indicating that the infection of p-hepatocytes by SDA-1 was mediated through CXCR4.

A previous study [19] reported that the HIV-1 gp120 *env* directly caused hepatocyte death by signaling through CXCR4 *in vitro*; however, most studies were performed using the hepatoma Huh-7 cells not hepatocytes, therefore, it may not really reflect the nature of liver damage. To explore the pathological effects of HIV-1 CD4-independent infection on hepatocytes, we exposed p-hepatocytes to the SDA-1 and analyzed cell viability. We found that the viability of the p-hepatocytes in cells cultured with or without SDA-1 Env-chimeric viruses was comparable (96%, *P* was not significant) indicating that HIV-1 CD4-independent infection rarely induces hepatocyte death via an apoptotic process (data not shown). To further examine whether the infection or replication of SDA-1 is limited only to a certain number of p-hepatocytes or whether the infectivity or replication is influenced by the cell cycle, we studied the intracellular expression by flow cytometry of p24 and Ki-67 [43], a marker strictly associated with cell proliferation, in the HIV-1-infected p-hepatocytes. As shown in Fig. 4d, we found that 32.49% of p-hepatocytes were infected by SDA-1. However, there was no significant difference in

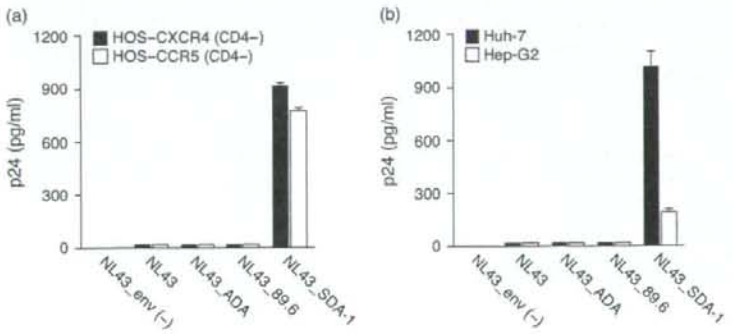

Fig. 3. CD4-independent infection of SDA-1 Env-chimeric viruses. The HOS cells (CD4⁻) expressing either CXCR4 or CCR5 (a) and two CD4⁻ human hepatoma cells (b) were incubated with the indicated HIV-1 Env-chimeric viruses. Virus replication was then monitored by p24 antigen production on day 3. Results shown (a, b) are means of triplicate experiments. Bars, standard deviation.

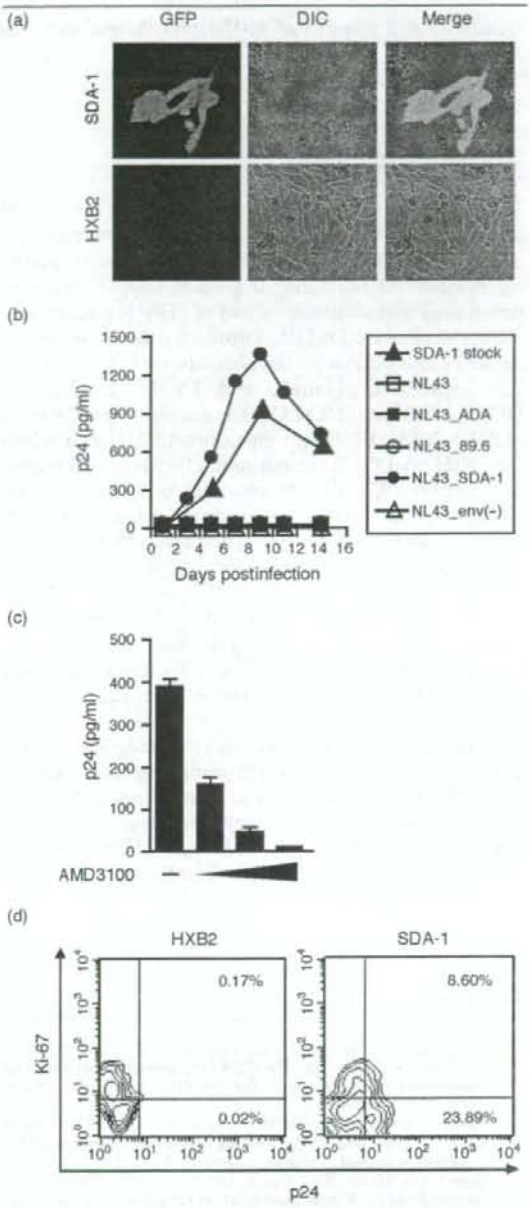

Fig. 4. SDA-1 enters and replicates in CD4$^-$ human p-hepatocytes. (a) Entry of SDA-1 into p-hepatocytes. The p-hepatocytes were exposed to the indicated HIV-1 GFP-p viruses for 48 h. Infectivity was determined as GFP$^+$ cells by confocal microscopy. (b) Replication of SDA-1 Env-chimeric viruses and SDA-1 virus stock in human p-hepatocytes. (c) SDA-1 infects p-hepatocytes through CXCR4. The inhibitory effects of AMD 3100 (0.1, 0.3 and 1.0 μM) on SDA-1 Env-chimeric viruses infection of p-hepatocytes were studied. Results shown are means of triplicate experiments. Bars, SD. (d) SDA-1 replicates in both proliferating and static human p-hepatocytes. Intracellular stainings of HIV-1-infected p-hepatocytes for p24 and Ki-67 were analyzed by flow cytometry. CXCR4, chemokine (C-X-C motif) receptor 4; GFP-p, GFP-pseudotypes.

percentage of p24 expression between Ki-67$^+$ (31%) and Ki-67$^-$ p-hepatocytes (33.1%), suggesting that SDA-1 efficiently enters and replicates in both proliferating and static hepatocytes.

Considering that SDA-1 can infect hepatocytes *in vitro*, it would have been interesting to determine whether the patient's liver was infected *in vivo*. However, consent for a liver biopsy was denied by the patient's family. There was no evidence of liver dysfunction. When virus was isolated from this patient; however, liver damage [an aspartate aminotransferase (AST)/alanine aminotransferase (ALT) ratio $\geq$1] was observed at the end of the clinical stage. Although the cause of liver injury was unclear, our present data suggest that CD4-independent HIV-1 infection may lead to hepatocellular damage.

Discussion

In this study, we characterized a quasispecies of a CD4-independent HIV-1 isolate, termed SDA-1, which was able to utilize either CXCR4 or CCR5 in the absence of CD4. Moreover, we demonstrated that SDA-1 efficiently entered and replicated in Huh-7 hepatoma cells and normal human hepatocytes, through CXCR4, without inducing apoptotic cell death.

Many SIV and HIV-2 isolates can infect cells without CD4, at least to some extent. However, CD4-independent HIV-1 viruses have been rarely isolated and, so far, only a few laboratory-adapted CD4-independent HIV-1 variants have been reported. It must be noted that CD4-independent HIV-1 variants, isolated *in vitro* by passage through cells lacking CD4, have been shown to be more sensitive to neutralizing antibodies than CD4-dependent viruses [44,45]. Therefore, we might hypothesize that the emergence of a quasispecies of HIV-1 with a reduced requirement for CD4 is likely to be at a low abundance relative to the more common CD4$^+$ strains. However, with disease progression, HIV-1 variants with reduced affinity for CD4 and with increased affinity for chemokine receptor could evolve and become more robust in the viral quasispecies, disseminate in a variety of CD4$^-$ tissues *in vivo* under conditions of both reduced immunological pressure and a dramatically reduced pool of target CD4$^+$ cells concomitant with high levels of virus replication. It will be important to search the viral quasispecies in other patients, especially in the later stages of HIV-1 disease for the existence of similar CD4-independent HIV-1 variants and expanded cellular tropism.

Fig. 4. (Continued)

Although the extent to which $CD4^-$ cells are infected *in vivo* is unclear, it has been widely thought to be low. Nonetheless, recent studies [11,12] utilizing the novel approach of laser capture microscopy have revealed HIV-1 sequences in isolated $CD4^-$ cells of kidney epithelium and neuronal cells, indicating that latent infection might occur in such cells or tissues *in vivo*. The mechanism of viral entry into $CD4^-$ cells remains unclear, but as we show here the evidence of emergence of CD4-independent strains *in vivo* must be kept in mind.

End-stage liver disease is now becoming a frequent cause of death in HIV-1-infected hospitalized patients. HCV and HBV coinfection with HIV-1 has been shown to enhance the progression of liver damage [16]. However, little attention has been given to the direct virological interaction between HIV and HCV/HBV in the liver, as HIV has been thought not to infect hepatocytes directly. Nonetheless, a number of reports have documented that histological liver abnormalities occurred solely as a result of HIV-1 infection. In our study, we clearly demonstrated that SDA-1 efficiently enters and replicates in both proliferating and static hepatocytes through CXCR4. To our knowledge, this is the first report that HIV-1 can efficiently replicate in normal hepatocytes. Furthermore, we have shown that HIV-1 infection did not induce significant cytocidal effects in the hepatocytes. It is noteworthy that the liver is a continuously regenerating organ. Therefore, if HIV-1 enters and integrates its DNA into the host genome, liver cells containing HIV-1 DNA will be continuously generated by the division of the infected cells. Thus, the expression of HIV-1 proteins on the infected cell surface might result in chronic damage of the liver cells by inducing host immune responses. Direct virological interaction between HIV, HCV and HBV in the liver or enhanced production of HIV-1 by inflammatory cytokines produced by the HCV and HBV-activated immune cells might also exacerbate the liver injury. At present, however, we have no definite information concerning the extent to which patients' hepatocytes harbor HIV-1 and CD4-independent HIV-1 variants.

Finally, a particularly important area of vaccine research is to take advantage of gp120 structural information to guide the design of novel envelope immunogens. As has been reported, CD4-dependent viruses hide neutralizing epitopes and only CD4 binding to gp120 induces conformational changes in gp120 to fully expose epitopes for broadly neutralizing antibodies. The CD4-independent strain we isolated here seems particularly important, as it can efficiently replicate in $CD4^-$ hepatocytes. Therefore, the gp120 structural alterations, which might expose the coreceptor binding site without binding to CD4, may also open up other sites that could yield neutralizing antibodies. Nevertheless, evidence of a clinical CD4-independent R5X4 HIV-1 virus should have important implications concerning the range of mutability and tropism of HIV-1 and the pathogenesis of AIDS.

Acknowledgements

We would like to thank Dr Shinji Okada for the clinical data of this patient. We also thank to Dr Y. Koyanagi, Dr T. Hara, Dr R. Furuta and H. Sakai for technical supports for isolation of the virus, sequences analysis, cell–cell fusion assay and chimeric viruses of SDA-1, respectively. We are indebted to Dr D.R. Littman for the gift of HIV-1 luciferase and GFP reporter plasmids, Dr C.D. Weiss for Env expression plasmids, and Dr N. Laudau for HOS.CXCR4 and HOS.CCR5 cells. We thank Division of AIDS, NIAID, NIH for providing AMD3100 through the NIH AIDS Research and Reference Reagent Programme. We also thank Takeda Pharmaceutical Company Ltd. (Osaka, Japan) for providing TAK-779. We are grateful for Dr M. Robert-Guroff for critical reading of the manuscript.

The present work was supported by Grant-in-Aid for Scientific Research B from JSPS and the Scientific Research Expenses for Health and Welfare Programme from the Ministry of Health and Welfare, Japan.

P.X., H.L., Y.S. and T.H. designed the study. P.X., O.U., Y.S., M.Z., Y.A. and H.G. performed the experiments. P.X., O.U, Y.S., H.L. and T.H. analyzed the data. N.S. and H.H. contributed to the coreceptor expressing cell lines. P.X., H.L., Y.S., O.U., N.S., H.H. and T.H. contributed to writing the paper. T.H. contributed to grant application and financial support.

References

1. Dalgleish AG, Beverley PC, Clapham PR, Crawford DH, Greaves MF, Weiss RA. **The CD4 (T4) antigen is an essential component of the receptor for the AIDS retrovirus.** *Nature* 1984; **312**:763–767.
2. Feng Y, Broder CC, Kennedy PE, Berger EA. **HIV-1 entry cofactor: functional cDNA cloning of a seven-transmembrane, G protein-coupled receptor.** *Science* 1996; **272**:872–877.
3. Berger EA, Doms RW, Fenyo EM, Korber BT, Littman DR, Moore JP, *et al.* **A new classification for HIV-1.** *Nature* 1998; **391**:240.
4. Berger EA, Murphy PM, Farber JM. **Chemokine receptors as HIV-1 coreceptors: roles in viral entry, tropism, and disease.** *Annu Rev Immunol* 1999; **17**:657–700.
5. Edinger AL, Mankowski JL, Doranz BJ, Margulies BJ, Lee B, Rucker J, *et al.* **CD4-independent, CCR5-dependent infection of brain capillary endothelial cells by a neurovirulent simian immunodeficiency virus strain.** *Proc Natl Acad Sci USA* 1997; **94**:14742–14747.
6. Reeves JD, Hibbitts S, Simmons G, McKnight A, Azevedo-Pereira JM, Moniz-Pereira J, Clapham PR. **Primary human immunodeficiency virus type 2 (HIV-2) isolates infect CD4-negative cells via CCR5 and CXCR4: comparison with HIV-1 and simian immunodeficiency virus and relevance to cell tropism in vivo.** *J Virol* 1999; **73**:7795–7804.

7. Dumonceaux J, Nisole S, Chanel C, Quivet L, Amara A, Baleux F, *et al.* **Spontaneous mutations in the env gene of the human immunodeficiency virus type 1 NDK isolate are associated with a CD4-independent entry phenotype.** *J Virol* 1998; **72**:512–519.
8. Hoffman TL, LaBranche CC, Zhang W, Canziani G, Robinson J, Chaiken I, *et al.* **Stable exposure of the coreceptor-binding site in a CD4-independent HIV-1 envelope protein.** *Proc Natl Acad Sci USA* 1999; **96**:6359–6364.
9. Kolchinsky P, Mirzabekov T, Farzan M, Kiprilov E, Cayabyab M, Mooney LJ, *et al.* **Adaptation of a CCR5-using, primary human immunodeficiency virus type 1 isolate for CD4-independent replication.** *J Virol* 1999; **73**:8120–8126.
10. Zerhouni B, Nelson JA, Saha K. **Isolation of CD4-independent primary human immunodeficiency virus type 1 isolates that are syncytium inducing and acutely cytopathic for CD8+ lymphocytes.** *J Virol* 2004; **78**:1243–1255.
11. Torres-Munoz J, Stockton P, Tacoronte N, Roberts B, Maronpot RR, Petito CK. **Detection of HIV-1 gene sequences in hippocampal neurons isolated from postmortem AIDS brains by laser capture microdissection.** *J Neuropathol Exp Neurol* 2001; **60**:885–892.
12. Marras D, Bruggeman LA, Gao F, Tanji N, Mansukhani MM, Cara A, *et al.* **Replication and compartmentalization of HIV-1 in kidney epithelium of patients with HIV-associated nephropathy.** *Nat Med* 2002; **8**:522–526.
13. Cao YZ, Dieterich D, Thomas PA, Huang YX, Mirabile M, Ho DD. **Identification and quantitation of HIV-1 in the liver of patients with AIDS.** *AIDS* 1992; **6**:65–70.
14. Housset C, Lamas E, Brechot C. **Detection of HIV1 RNA and p24 antigen in HIV1-infected human liver.** *Res Virol* 1990; **141**:153–159.
15. Bica I, McGovern B, Dhar R, Stone D, McGowan K, Scheib R, Snydman DR. **Increasing mortality due to end-stage liver disease in patients with human immunodeficiency virus infection.** *Clin Infect Dis* 2001; **32**:492–497.
16. Martin-Carbonero L, Soriano V, Valencia E, Garcia-Samaniego J, Lopez M, Gonzalez-Lahoz J. **Increasing impact of chronic viral hepatitis on hospital admissions and mortality among HIV-infected patients.** *AIDS Res Hum Retroviruses* 2001; **17**:1467–1471.
17. Sabin CA. **The changing clinical epidemiology of AIDS in the highly active antiretroviral therapy era.** *AIDS* 2002; **16 Suppl 4**:S61–S68.
18. Lefkowitch JH. **Pathology of AIDS-related liver disease.** *Dig Dis* 1994; **12**:321–330.
19. Vlahakis SR, Villasis-Keever A, Gomez TS, Bren GD, Paya CV. **Human immunodeficiency virus-induced apoptosis of human hepatocytes via CXCR4.** *J Infect Dis* 2003; **188**:1455–1460.
20. **Centers for Disease Control and Prevention: 1993 revised classification system for HIV infection and expanded surveillance case definition for AIDS among adolescents and adults.** [No. RR-17] *MMWR Morb Mortal Wkly Rep* 1992; **41**:1–19.
21. Wei X, Decker JM, Wang S, Hui H, Kappes JC, Wu X, *et al.* **Antibody neutralization and escape by HIV-1.** *Nature* 2003; **422**:307–312.
22. Derdeyn CA, Decker JM, Bibollet-Ruche F, Mokili JL, Muldoon M, Denham SA, *et al.* **Envelope-constrained neutralization-sensitive HIV-1 after heterosexual transmission.** *Science* 2004; **303**:2019–2022.
23. Liu SL, Rodrigo AG, Shankarappa R, Learn GH, Hsu L, Davidov O, *et al.* **HIV quasispecies and resampling.** *Science* 1996; **273**:415–416.
24. Shankarappa R, Margolick JB, Gange SJ, Rodrigo AG, Upchurch D, Farzadegan H, *et al.* **Consistent viral evolutionary changes associated with the progression of human immunodeficiency virus type 1 infection.** *J Virol* 1999; **73**:10489–10502.
25. Thompson JD, Higgins DG, Gibson TJ. **CLUSTAL W: improving the sensitivity of progressive multiple sequence alignment through sequence weighting, position-specific gap penalties and weight matrix choice.** *Nucl Acids Res* 1994; **22**:4673–4680.
26. Gerhardt M, Mloka D, Tovanabutra S, Sanders-Buell E, Hoffmann O, Maboko L, *et al.* **In-depth, longitudinal analysis of viral quasispecies from an individual triply infected with late-stage human immunodeficiency virus type 1, using a multiple PCR primer approach.** *J Virol* 2005; **79**:8249–8261.
27. Liu HY, Soda Y, Shimizu N, Haraguchi Y, Jinno A, Takeuchi Y, Hoshino H. **CD4-Dependent and CD4-independent utilization of coreceptors by human immunodeficiency viruses type 2 and simian immunodeficiency viruses.** *Virology* 2000; **278**:276–288.
28. Landau NR, Littman DR. **Packaging system for rapid production of murine leukemia virus vectors with variable tropism.** *J Virol* 1992; **66**:5110–5113.
29. Nakabayashi H, Taketa K, Miyano K, Yamane T, Sato J. **Growth of human hepatoma cells lines with differentiated functions in chemically defined medium.** *Cancer Res* 1982; **42**:3858–3863.
30. Hendrix CW, Flexner C, MacFarland RT, Giandomenico C, Fuchs EJ, Redpath E, *et al.* **Pharmacokinetics and safety of AMD-3100, a novel antagonist of the CXCR-4 chemokine receptor, in human volunteers.** *Antimicrob Agents Chemother* 2000; **44**:1667–1673.
31. Baba M, Nishimura O, Kanzaki N, Okamoto M, Sawada H, Iizawa Y, *et al.* **A small-molecule, nonpeptide CCR5 antagonist with highly potent and selective anti-HIV-1 activity.** *Proc Natl Acad Sci USA* 1999; **96**:5698–5703.
32. He J, Chen Y, Farzan M, Choe H, Ohagen A, Gartner S, *et al.* **CCR3 and CCR5 are co-receptors for HIV-1 infection of microglia.** *Nature* 1997; **385**:645–649.
33. Connor RI, Chen BK, Choe S, Landau NR. **Vpr is required for efficient replication of human immunodeficiency virus type-1 in mononuclear phagocytes.** *Virology* 1995; **206**:935–944.
34. Reiser J. **Production and concentration of pseudotyped HIV-1-based gene transfer vectors.** *Gene Ther* 2000; **7**:910–913.
35. Li SL, Zhang XY, Ling H, Ikeda J, Shirato K, Hattori T. **A VSV-G pseudotyped HIV vector mediates efficient transduction of human pulmonary artery smooth muscle cells.** *Microbiol Immunol* 2000; **44**:1019–1025.
36. Adachi A, Gendelman HE, Koenig S, Folks T, Willey R, Rabson A, Martin MA. **Production of acquired immunodeficiency syndrome-associated retrovirus in human and nonhuman cells transfected with an infectious molecular clone.** *J Virol* 1986; **59**:284–291.
37. Furuta RA, Wild CT, Weng Y, Weiss CD. **Capture of an early fusion-active conformation of HIV-1 gp41.** *Nat Struct Biol* 1998; **5**:276–279.
38. Sattentau QJ, Dalgleish AG, Weiss RA, Beverley PC. **Epitopes of the CD4 antigen and HIV infection.** *Science* 1986; **234**:1120–1123.
39. Saha K, Zhang J, Gupta A, Dave R, Yimen M, Zerhouni B. **Isolation of primary HIV-1 that target CD8+ T lymphocytes using CD8 as a receptor.** *Nat Med* 2001; **7**:65–72.
40. Brass AL, Dykxhoorn DM, Benita Y, Yan N, Engelman A, Xavier RJ, *et al.* **Identification of host proteins required for HIV infection through a functional genomic screen.** *Science* 2008; **319**:921–926.
41. Cormier EG, Tsamis F, Kajumo F, Durso RJ, Gardner JP, Dragic T. **CD81 is an entry coreceptor for hepatitis C virus.** *Proc Natl Acad Sci USA* 2004; **101**:7270–7274.
42. Jopling CL, Yi M, Lancaster AM, Lemon SM, Sarnow P. **Modulation of hepatitis C virus RNA abundance by a liver-specific MicroRNA.** *Science* 2005; **309**:1577–1581.
43. Harrison RF, Rowlands DC. **Proliferating cell nuclear antigen as a marker of hepatocyte proliferation.** *Lancet* 1994; **343**:1290–1291.
44. Edwards TG, Hoffman TL, Baribaud F, Wyss S, LaBranche CC, Romano J, *et al.* **Relationships between CD4 independence, neutralization sensitivity, and exposure of a CD4-induced epitope in a human immunodeficiency virus type 1 envelope protein.** *J Virol* 2001; **75**:5230–5239.
45. Kolchinsky P, Kiprilov E, Sodroski J. **Increased neutralization sensitivity of CD4-independent human immunodeficiency virus variants.** *J Virol* 2001; **75**:2041–2050.

CLINICAL AND VACCINE IMMUNOLOGY, Mar. 2008, p. 544–548 Vol. 15, No. 3
1556-6811/08/$08.00+0 doi:10.1128/CVI.00355-07

Increased Synthesis of Anti-Tuberculous Glycolipid Immunoglobulin G (IgG) and IgA with Cavity Formation in Patients with Pulmonary Tuberculosis▽

Masako Mizusawa,[1]¶ Mizuoho Kawamura,[2] Mikio Takamori,[3] Tetsuya Kashiyama,[3] Akira Fujita,[3] Motoki Usuzawa,[1] Hiroki Saitoh,[1] Yugo Ashino,[1] Ikuya Yano,[4] and Toshio Hattori[1]*

Division of Emerging Infectious Diseases, Graduate School of Medicine, Tohoku University, Sendai, Miyagi 980-8574,[1] Fuji Research Laboratories, Kyowa Medex, Co., Ltd., Shizuoka 411-0932,[2] Department of Respiratory Diseases, Tokyo Metropolitan Fuchu Hospital, Fuchu, Tokyo 183-8524,[3] and Japan BCG Central Laboratory, Kiyose, Tokyo 204-0022,[4] Japan

Received 23 August 2007/Returned for modification 24 September 2007/Accepted 19 December 2007

Tuberculous glycolipid (TBGL) antigen is a cell wall component of *Mycobacterium tuberculosis* and has been used for the serodiagnosis of tuberculosis. We investigated correlations between the levels of anti-TBGL antibodies and a variety of laboratory markers that are potentially influenced by tuberculous infection. Comparisons between patients with cavitary lesions and those without cavitary lesions were also made in order to determine the mechanism underlying the immune response to TBGL. Blood samples were obtained from 91 patients with both clinically and microbiologically confirmed active pulmonary tuberculosis (60 male and 31 female; mean age, 59 ± 22 years old). Fifty-nine patients had cavitary lesions on chest X-rays. Positive correlations were found between anti-TBGL immunoglobulin G (IgG) and C-reactive protein (CRP) ($r = 0.361$; $P < 0.001$), between anti-TBGL IgA and soluble CD40 ligand (sCD40L) ($r = 0.404$; $P < 0.005$), between anti-TBGL IgG and anti-TBGL IgA ($r = 0.551$; $P < 0.0000005$), and between anti-TBGL IgM and serum IgM ($r = 0.603$; $P < 0.00000005$). The patients with cavitary lesions showed significantly higher levels of anti-TBGL IgG ($P < 0.005$), anti-TBGL IgA ($P < 0.05$), white blood cells ($P < 0.01$), neutrophils ($P < 0.005$), basophils ($P < 0.0005$), natural killer cells ($P < 0.05$), CRP ($P < 0.0005$), KL-6 (sialylated carbohydrate antigen KL-6) ($P < 0.0005$), IgA ($P < 0.05$), and sCD40L ($P < 0.01$). The observed positive correlations between the anti-TBGL antibody levels and inflammatory markers indicate the involvement of inflammatory cytokines and NKT cells in the immunopathogenesis of pulmonary tuberculosis.

There were an estimated 8.8 million new tuberculosis (TB) cases in 2005. TB incidence reached a peak worldwide, but the total number of new TB cases is still rising. The numbers of human immunodeficiency virus (HIV)-positive and multidrug-resistant TB patients diagnosed and treated are increasing (22). To develop new drugs and vaccines against TB, it is essential to study its immunopathogenesis. Lipoarabinomannnan (LAM), a complex glycolipid, is a major cell wall component of *Mycobacterium tuberculosis*. It has been researched extensively as an immunomodulator (4, 7, 9, 24, 26). LAM has also been used as a glycolipid antigen in the serodiagnostic method for TB. In addition to LAM, there are many glycolipids constituting the mycobacterial cell wall, such as trehalose 6,6-dimycolate (TDM). We used TDM, a glycolipid antigen purified from *Mycobacterium tuberculosis* H37Rv, in an enzyme-linked immunosorbent assay (ELISA) and reported that its sensitivity was 81% and its specificity was 96% (14). Subsequently, by combining TDM with more hydrophobic glycolipids, a new tuberculous glycolipid (TBGL) antigen was designed and a more sensitive serodiagnostic kit for TB, an anti-TBGL immunoglobulin G (IgG) test, was developed (11). Although TBGL has been used as a serodiagnostic antigen for TB and its clinical evaluations have been reported in several studies, how TBGL is involved in tuberculous pathogenesis has not been studied. Since TBGL is one of the cell wall components of *Mycobacterium tuberculosis*, like LAM, it may have some important roles in the immunopathogenesis of TB, as does LAM. In order to determine the mechanism underlying the immune response to TBGL, we measured plasma IgA, IgM, and IgG titers specific for TBGL and investigated correlations between those antibody titers and laboratory markers potentially influenced by TB infection in patients with active pulmonary TB. The measured markers were the numbers of white blood cells with differential counts, CD3-positive lymphocytes (T cells), CD20-positive lymphocytes (B cells), and CD56-positive lymphocytes (natural killer cells) and levels of serum IgG, serum IgA, serum IgM, serum albumin, serum creatinine, serum C-reactive protein (CRP), plasma soluble CD40 ligand (sCD40L), and plasma KL-6 (sialylated carbohydrate antigen KL-6). KL-6 is a mucinous high-molecular-weight glycoprotein expressed on type II pneumocytes, and it was reported to be elevated in the sera of patients with interstitial pneumonia (13). We used plasma samples, but the level of KL-6 is known to show no significant difference between serum and plasma. We measured KL-6 because TB patients with extensive radiographic changes were also reported to have higher KL-6 values (8).

* Corresponding author. Mailing address: Division of Emerging Infectious Diseases, Graduate School of Medicine, Tohoku University, 1-1 Seiryo-cho, Aoba-ku, Sendai, Miyagi, Japan 980-8574. Phone: 81-227178220. Fax: 81-227178221. E-mail: hattori.t@rid.med.tohoku.ac.jp.

¶ Present address: Jichi Medical University Hospital, 3311-1 Yakushiji, Shimotsuke-shi, Tochigi 329-0498, Japan.

▽ Published ahead of print on 9 January 2008.

CD40L is expressed on the surfaces of activated $CD4^+$ T cells, basophils, and mast cells. The binding of CD40L to its receptor, CD40, on the surfaces of B cells stimulates B-cell proliferation, adhesion, and differentiation. A soluble isoform of CD40L has been shown to exist in the circulation, exhibiting full activity in B-cell proliferation and differentiation assays (16). It was reported that the treatment of wild-type CD40 mice with sCD40L fusion protein elicited a pulmonary inflammatory response that was not observed in identically treated CD40 knockout mice (21). Based on these reports, we measured sCD40L as a possible marker of pulmonary inflammation.

Furthermore, it was reported that the positive rate and the titers of anti-TBGL IgG were higher in pulmonary TB patients with cavitary lesions than in those without cavitary lesions (15). Considering this result, we subdivided the patients into two groups, those with cavitary lesions ($cavity^+$ group) and those without cavitary lesions ($cavity^-$ group), and compared multiple laboratory markers to determine associations.

In addition, we categorized the patients into three groups based on chest X-ray findings, namely, minimal, moderately advanced, and far advanced, according to the classification of the National Tuberculosis and Respiratory Disease Association of the USA (NTA) (6), and compared all the measured laboratory markers, including anti-TBGL antibodies, among the three groups to determine if there were any parameters related to disease progression and severity.

MATERIALS AND METHODS

Subjects. We designed a cross-sectional study using 121 patients at Tokyo Metropolitan Fuchu Hospital between May 2004 and August 2005. These patients were clinically diagnosed as having active TB and admitted to the hospital for treatment. Medical histories were taken from the enrolled patients, and all of them underwent physical examination, chest X-rays, blood test and culture test for acid-fast bacilli, and/or TB-PCR test of sputum samples. Ninety-one subjects were selected (60 males and 31 females; mean age [± standard deviation], 59 ± 22 years old) for analysis according to the following criteria: (i) diagnosed as having pulmonary TB by positive culture or positive PCR for *Mycobacterium tuberculosis* in sputum, (ii) untreated or undergoing less than 2 weeks of TB treatment, (iii) negative for *Mycobacterium avium* complex infection, (iv) negative for HIV infection, (v) no malignancy, and (vi) no other active pulmonary diseases. The remaining 30 patients were excluded for the following reasons: 4 for both negative culture and a negative PCR test for *Mycobacterium tuberculosis* in sputum, 5 for more than 2 weeks of TB treatment, 2 for *Mycobacterium avium* complex infection, 4 for HIV infection, 3 for malignancy, 2 for interstitial pneumonia, and 10 for insufficient data collection. We enrolled patients with less than 2 weeks of treatment based on a report that anti-TBGL IgG did not decrease until 1 month after the commencement of chemotherapy (15). The study was approved by the Ethics Committee of Tokyo Metropolitan Fuchu Hospital. We obtained written informed consent from all the enrolled patients.

TBGL antibody. Anti-TBGL antibodies were measured using a Determiner TBGL antibody ELISA kit (Kyowa Medex, Tokyo, Japan), an in vitro ELISA for the quantitative measurement of anti-TBGL IgG antibody in serum or plasma. This assay employs glycolipid antigens purified from *Mycobacterium tuberculosis* H37Rv (TBGL antigen) coated on a 96-well plate. The details of the assay were described in our previous studies (2, 11), but briefly, plasma was diluted 41-fold and added to wells that bound TBGL antigen. The wells were washed, and horseradish peroxidase-conjugated rabbit anti-human IgG, IgA, and IgM, all of which are specific to each heavy chain (Dako Japan, Kyoto, Japan), were added, followed by 60 min of incubation at room temperature. The plates were washed three times with washing buffer, 100 μl of TMBZ (3,3′,5,5′-tetramethylbenzidine) solution was added to each well, and the plates were incubated for 15 min at room temperature. To stop the enzyme reaction, 100 μl of 1 M H_2SO_4 was added, and the absorbance at 450 nm was measured with an MTP-120 plate reader (Corona Electric Co., Tokyo, Japan). The antibody titer was expressed according to a cutoff index. We scored the sample as positive when the titer was above the cutoff index for anti-TBGL IgG of 2.0 U/ml, the cutoff point proposed by Kishimoto et al. for the screening of patients with TB based on the diagnostic efficiency by receiver operating characteristic curve analysis (12). The cutoff values for anti-TBGL IgA and IgM are not available.

TABLE 1. Health status of patients in the study

Parameter	Value for group		
	Total	$Cavity^+$	$Cavity^-$
No. of patients	91	59	32
Age (yrs [mean ± SD])	59 ± 22	56 ± 21	64 ± 22
Gender (no. of males/no. of females)	60/31	42/17	18/14
No. of patients with history of:			
TB	20	14	6
Gastrectomy	3	3	3
Diabetes mellitus	14	7	7
Chronic renal failure	5	2	3
Diabetes mellitus and chronic renal failure	1	0	1

Measured laboratory markers. We investigated the correlations between anti-TBGL antibodies and laboratory markers of TB infection, including immunocompetent cells. We measured the number of white blood cells with differential counts and the numbers of lymphocytes positive for CD3, CD20, and CD56 by FACSCalibur flow cytometry (Becton Dickinson and Company, NJ), using phycoerythrin-conjugated Leu-4 monoclonal antibody (MAb), fluorescein isothiocyanate-conjugated Leu-16 MAb, and phycoerythrin-conjugated Leu-19 MAb, respectively (Becton Dickinson and Company, NJ). Serum albumin and serum creatinine were measured because malnutrition and chronic renal failure are major risk factors for TB infection. We also measured IgA, IgG, IgM, and CRP by using serum and sCD40L and KL-6 by using plasma. The rationales for measuring sCD40L and KL-6 were stated in the introduction. sCD40L and KL-6 ELISA kits were purchased from Medsystems Diagnostics (Vienna, Austria) and from Sanko-Junyaku (Tokyo, Japan), respectively. The titers were measured according to the manufacturers' protocols.

Radiographic classification. We subdivided the patients into two groups, the $cavity^+$ group and the $cavity^-$ group. We also categorized the patients into three groups based on chest X-ray findings, namely, minimal, moderately advanced, and far advanced, according to the classification of the NTA. Minimal lesions include those that are of slight to moderate density but do not contain demonstrable cavitation. They may involve a small part of one or both lungs, but the total extent, regardless of distribution, should not exceed the volume of lung on one side which is present above the second chondrosternal junction and the spine of the fourth or the body of the fifth thoracic vertebra. Moderately advanced lesions may be present in one or both lungs, but the total extent should not exceed the following limits: disseminated lesions of slight to moderate density may extend throughout the total volume of one lung or the equivalent in both lungs; dense and confluent lesions must be limited in extent to one-third the volume of one lung; and the total diameter of cavitation, if present, must be less than 4 cm. Far advanced lesions are more extensive than moderately advanced lesions (6).

Statistical analysis. Laboratory data were analyzed using Stat Flex, version 5 (Artec, Osaka, Japan), and Statcel 2 (OMS Publishing Inc., Saitama, Japan). Correlations between levels of each parameter were evaluated by Spearman's rank correlation coefficient. The significances of differences were evaluated by the Mann-Whitney test. P values of <0.05 were considered significant. Bonferroni adjustment was used for multiple comparisons.

RESULTS

Health status of patients and positive rate. The health status of the included patients is shown in Table 1. Among the 91 patients in this study, there were 20 patients with histories of TB, 3 patients with histories of gastrectomy, 14 patients with diabetes mellitus, 5 patients with chronic renal failure, and 1 patient with both diabetes mellitus and chronic renal failure. Fifty-nine patients had cavitary lesions on chest X-rays. The positive rate for the anti-TBGL IgG test, a commercialized

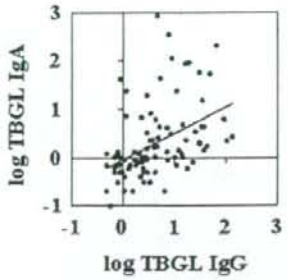

FIG. 1. Correlation between anti-TGBL IgG (TBGL IgG) and anti-TBGL IgA (TBGL IgA) ($r = 0.551$; $P < 0.0000005$).

diagnostic test for TB, was 79.7% (47/59 patients) for the cavity$^+$ group, 50% (16/32 patients) for the cavity$^-$ group, and 69.2% (63/91 patients) overall. No patient was on steroid therapy.

Correlations between anti-TBGL antibodies. We sought correlations between each of the anti-TBGL antibodies. Anti-TBGL IgG had a positive correlation with anti-TBGL IgA ($r = 0.551$; $P < 0.0000005$) (Fig. 1). No other correlations were shown between the anti-TBGL antibodies.

Correlations between anti-TBGL antibodies and influential laboratory markers. Anti-TBGL IgG had positive correlations with IgA ($r = 0.228$; $P < 0.05$), CRP ($r = 0.361$; $P < 0.001$), and KL-6 ($r = 0.275$; $P < 0.01$) and negative correlations with creatinine ($r = -0.249$; $P < 0.05$) and albumin ($r = -0.240$; $P < 0.05$). Anti-TBGL IgA had positive correlations with IgG ($r = 0.285$; $P < 0.01$), IgA ($r = 0.300$; $P < 0.005$), KL-6 ($r = 0.225$; $P < 0.05$), and sCD40L ($r = 0.404$; $P < 0.005$). Anti-TBGL IgM had positive correlations with IgM ($r = 0.603$; $P < 0.00000005$) and albumin ($r = 0.251$; $P < 0.05$).

TABLE 2. Measured parameters (mean ± SD) and comparison between cavity* group and cavity$^-$ group

Parameter	Value for group			*P* value*
	Total	Cavity$^+$	Cavity$^-$	
TBGL-IgG (U/ml)	13.2 ± 23.5	17.1 ± 27.6	6.0 ± 9.9	<0.005*
TBGL-IgA (U/ml)	22.6 ± 95.4	32.0 ± 117.2	5.3 ± 15.7	<0.05*
TBGL-IgM (U/ml)	6.0 ± 5.6	5.9 ± 5.8	6.2 ± 5.3	NS
IgG (mg/dl)	1,518 ± 471	1,523 ± 510	1,509 ± 395	NS
IgA (mg/dl)	416 ± 213	451 ± 236	348 ± 140	<0.05*
IgM (mg/dl)	106 ± 57	103 ± 58	111 ± 55	NS
White blood cells/μl	7,236 ± 2,706	7,830 ± 3,020	6,141 ± 1,513	<0.01*
Neutrophils/μl	5,567 ± 2,532	6,192 ± 2,798	4,415 ± 1,362	<0.005*
Monocytes/μl	397 ± 223	424 ± 243	347 ± 172	NS
Eosinophils/μl	115 ± 119	126 ± 135	94 ± 80	NS
Basophils/μl	24 ± 45	22 ± 46	29 ± 43	<0.0005*
Lymphocytes/μl	1,128 ± 740	1,061 ± 766	1,253 ± 685	NS
CD3$^+$ cells/μl	751 ± 509	715 ± 517	815 ± 496	NS
CD20$^+$ cells/μl	131 ± 115	114 ± 93	161 ± 143	NS
CD56$^+$ cells/μl	208 ± 197	197 ± 223	231 ± 140	<0.05*
CRP (mg/dl)	4.5 ± 5.2	5.7 ± 5.8	2.2 ± 2.9	<0.0005*
KL-6 (U/ml)	564 ± 459	662 ± 518	382 ± 241	<0.0005*
sCD40L (ng/ml)	1.8 ± 2.5	2.1 ± 3.0	1.2 ± 1.0	<0.01*
Creatinine (mg/ml)	1.0 ± 1.5	0.8 ± 0.6	1.5 ± 2.4	NS
Albumin (g/dl)	3.4 ± 0.8	3.3 ± 0.7	3.6 ± 0.8	NS

* Asterisks show significant differences between the cavity$^+$ group and the cavity$^-$ group. NS, no significant difference. The significances of differences were evaluated by the Mann-Whitney test. *P* values of <0.05 were considered significant.

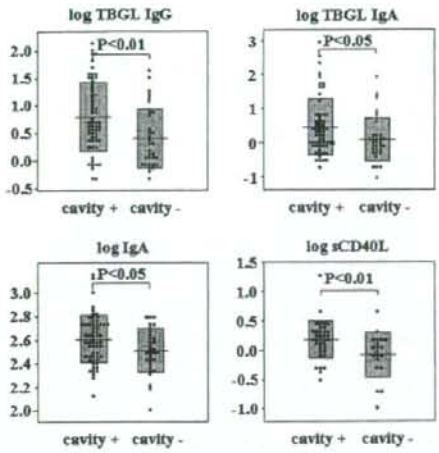

FIG. 2. Anti-TBGL IgG (TBGL IgG), anti-TBGL IgA (TBGL IgA), IgA, and sCD40L levels in cavity$^+$ and cavity$^-$ groups.

Comparison between patients with and without cavitary lesions. We compared all the measured laboratory markers between the patients with cavitary lesions (cavity$^+$ group) and those without cavitary lesions (cavity$^-$ group) in order to determine new differences apart from that of the anti-TBGL IgG level (15). As shown in Table 2, both anti-TBGL IgG and anti-TBGL IgA levels were significantly higher in the cavity$^+$ group ($P < 0.005$ and $P < 0.05$, respectively), but the anti-TBGL IgM titers showed no difference between the two groups. The numbers of white blood cells ($P < 0.001$), neutrophils ($P < 0.005$), basophils ($P < 0.0005$), and natural killer cells (CD56$^+$) ($P < 0.05$) were significantly higher in the cavity$^+$ group. The levels of CRP ($P < 0.0005$), KL-6 ($P < 0.0005$), IgA ($P < 0.05$), and sCD40L ($P < 0.01$) were also significantly higher in the cavity$^+$ group (Table 2; Fig. 2 and 3).

Radiographic changes and inflammatory markers. We compared the levels of the inflammatory markers CRP and KL-6

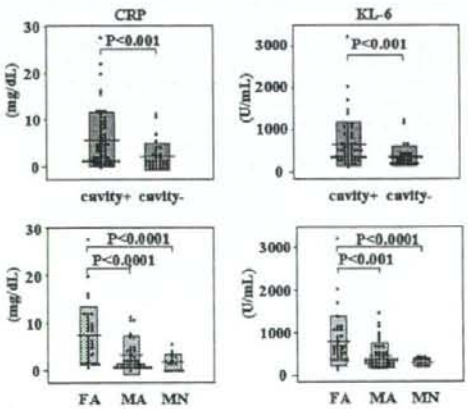

FIG. 3. CRP and KL-6 levels in cavity$^+$ and cavity$^-$ groups and NTA classification groups. FA, far advanced; MA, moderately advanced; MN, minimal.

among the three groups and found that the far advanced group had significantly higher levels of CRP and KL-6 than did the moderately advanced group ($P < 0.0001$ and $P < 0.0005$, respectively) or the minimal group ($P < 0.0001$ and $P < 0.00005$, respectively). Although no statistical significance appeared, CRP and KL-6 had a tendency to be higher in the moderately advanced group than in the minimal group (Fig. 3). However, there was no correlation between the levels of CRP and those of KL-6. No other parameters, including anti-TBGL antibodies, showed significant differences between the groups.

DISCUSSION

We report for the first time that the anti-TBGL IgG level correlates with the CRP level. This may not be surprising because CRP is a well-known inflammatory marker and inflammation is generally involved in antibody synthesis. However, the mechanism underlying the association between the anti-TBGL IgG level and CRP was not readily understandable. Trehalose 6,6′-dimycolate ("cord factor") is one of the principal antigens in TBGL, and cord factor has mycolic acid side chains. Mycolic acids are long-chain fatty acids that constitute the lipid-rich cell wall framework of mycobacteria, and their recognition is known to be mediated by CD1. Enomoto et al. discovered a CD1-restricted human T-cell line specific for glucose monomycolate, a glycosylated species of mycolic acids (5), and most CD1-restricted T cells are known to be natural killer T cells (NKT cells). Historical studies showed granuloma formation in the lungs of mice after intravenous administration of emulsified trehalose-6,6′-dimycolate ("cord factor") (23). The role of NKT cells in granuloma formation was also confirmed by the fact that granulomas were actually formed in wild-type mice injected with cell walls from *Mycobacterium tuberculosis* but not in Jα281$^-$ mice, which lack NKT cells (1). On the other hand, Mempel et al. demonstrated that NKT cells migrate to and accumulate at inflammatory sites and behave like inflammatory cells independently of the CD1 molecules (17), which could lead to the production of inflammatory markers such as CRP. The possibility of NKT-cell involvement in anti-TB immunity was also suggested in a recent study describing that NKT cells are selectively lower in the peripheral blood mononuclear cells of individuals with pulmonary TB (19). More extensive studies are necessary to clarify the relationship between TBGL and NKT cells in tuberculous granuloma formation.

The anti-TBGL IgA level was correlated with sCD40L. Wiley et al. reported that the treatment of wild-type CD40 mice with sCD40L fusion protein elicited a pulmonary inflammatory response that was not observed in identically treated CD40 knockout mice and that CD40 ligation could play an important role in the establishment of the inflammatory response (21). On the other hand, the expression of CD40L was reported to have a direct correlation with *Mycobacterium tuberculosis*-stimulated gamma interferon production by peripheral blood mononuclear cells (18). Since sCD40L is involved in both pulmonary inflammation and TB infection, it could play a role as an inflammatory marker in pulmonary TB. The correlation between the anti-TBGL IgA level and sCD40L may also reflect the following immunopathogenesis of *Mycobacterium tuberculosis* infection. In the cavity$^+$ group, sCD40L and IgA were significantly elevated. It is known that CD40 engagement by CD40L induces the production of endogenous transforming growth factor beta (TGF-β) and IgA secretion (25) and that TGF-β may be involved in the development and/or consequences of tuberculous granuloma formation (3). Therefore, the higher levels of sCD40L and IgA in the cavity$^+$ group may reflect the intense granuloma formation in cavitary lesions, and these immune responses may have led to the correlation of anti-TBGL IgA level and the sCD40L level.

The level of anti-TBGL IgG had a correlation with that of anti-TBGL IgA. This correlation was not due to cross-reaction of the secondary antibodies because unwanted antibodies had been removed by solid-phase absorption. Julián et al. conducted a comparative study of IgG, IgM, and IgA antibody responses to four trehalose-containing glycolipids, including cord factor, purified from *Mycobacterium tuberculosis* in the sera from 92 TB patients. They concluded that IgG antibody was more sensitive, IgA antibody was more specific, and IgM reactivity was negligible for all the glycolipid antigens used (10). Since TBGL is a glycolipid antigen containing cord factor, anti-TBGL IgA may yield a higher specificity than does anti-TBGL IgG, and the detection of both anti-TBGL IgG and anti-TBGL IgA may improve the diagnostic value. A prospective controlled study on anti-TBGL IgA will be necessary to confirm this possibility.

There was a strong correlation between the levels of anti-TBGL IgM and serum IgM. However, we concluded that this did not reflect specific immunity in TB infection because IgM has a low affinity and cross-reactivity in addition to its pentameric structure (20).

Inoue et al. reported that the serum levels of KL-6 in 57 patients with active pulmonary TB rose significantly according to the increase in the extent of radiographic findings based on the classification of the NTA, but there was no significant difference between those with cavities and those without cavities (8). In our study, the far advanced group had significantly higher levels of KL-6 than did the moderately advanced group and the minimal group, and although the difference was not statistically significant, the moderately advanced group had higher levels of KL-6 than did the minimal group. In contrast to Inoue's data, KL-6 was significantly higher in the cavity$^+$ group. The same results were shown for the level of CRP (Fig. 3), but no correlation was seen between KL-6 and CRP. Based on these findings, the level of KL-6 or CRP may reflect a different component of disease progression and could be used to evaluate the severity of pulmonary TB.

Although we found interesting correlations between anti-TBGL antibody levels and inflammatory markers, suggesting the involvement of inflammatory cytokines and NKT cells, confirmatory experiments have not been done, which is a major limitation of this study. Demonstrating specific immune responses to glycolipid antigens by using T cells from TB patients and their characterization would help to elucidate the immunopathogenesis of pulmonary TB.

ACKNOWLEDGMENTS

This work was supported by a special educational grant from the Ministry of Education, Culture Sports, Science and Technology and by a grant-in-aid from the Scientific Expenses for Health and Welfare

Program from the Ministry of Education, Culture Sports, Science and Technology.

We are grateful to T. Masunari for statistical analysis.

REFERENCES

1. **Apostolou, I., Y. Takahama, C. Belmant, T. Kawano, M. Huerre, G. Marchal, J. Cui, M. Taniguchi, H. Nakauchi, J. J. Fournie, P. Kourilsky, and G. Gachelin.** 1999. Murine natural killer T (NKT) cells [correction of natural killer cells] contribute to the granulomatous reaction caused by mycobacterial cell walls. Proc. Natl. Acad. Sci. USA **96:**5141–5146.
2. **Ashino, J., Y. Ashino, H. Guio, H. Saitoh, M. Mizusawa, and T. Hattori.** 2005. Low antibody response against tuberculous glycolipid (TBGL) in elderly gastrectomised tuberculosis patients. Int. J. Tuberc. Lung Dis. **9:** 1052–1053.
3. **Aung, H., Z. Toossi, S. M. McKenna, P. Gogate, J. Sierra, E. Sada, and E. A. Rich.** 2000. Expression of transforming growth factor-beta but not tumor necrosis factor-alpha, interferon-gamma and interleukin-4 in granulomatous lung lesions in tuberculosis. Tuber. Lung Dis. **80:**61–67.
4. **Chan, J., X. Fan, S. W. Hunter, P. J. Brennan, and B. R. Bloom.** 1991. Lipoarabinomannan, a possible virulence factor involved in persistence of *Mycobacterium tuberculosis* within macrophages. Infect. Immun. **59:**1755–1761.
5. **Enomoto, Y., M. Sugita, I. Matsunaga, T. Naka, A. Sato, T. Kawashima, K. Shimizu, H. Takahashi, Y. Norose, and I. Yano.** 2005. Temperature-dependent biosynthesis of glucose monomycolate and its recognition by CD1-restricted T cells. Biochem. Biophys. Res. Commun. **337:**452–456.
6. **Falk, A., J. B. O'Connor, and P. C. Pratt.** 1969. Classification of pulmonary tuberculosis, p. 68–76. *In* Diagnostic standards and classification of tuberculosis, 12th ed., vol. 6. National Tuberculosis and Respiratory Disease Association, New York, NY.
7. **Hunter, S. W., H. Gaylord, and P. J. Brennan.** 1986. Structure and antigenicity of the phosphorylated lipopolysaccharide antigens from the leprosy and tubercle bacilli. J. Biol. Chem. **261:**12345–12351.
8. **Inoue, Y., K. Nishimura, M. Shiode, H. Akutsu, H. Hamada, S. Fujioka, S. Fujino, A. Yokoyama, N. Kohno, and K. Hiwada.** 1995. Evaluation of serum KL-6 levels in patients with pulmonary tuberculosis. Tuber. Lung Dis. **76:** 230–233.
9. **Juffermans, N. P., A. Verbon, S. J. H. van Deventer, W. A. Buurman, H. Van Deutekom, P. Speelman, and T. van der Poll.** 1998. Serum concentrations of lipopolysaccharide activity-modulating proteins during tuberculosis. J. Infect. Dis. **178:**1839–1842.
10. **Julián, E., L. Matas, A. Perez, J. Alcaide, M. A. Laneelle, and M. Luquin.** 2002. Serodiagnosis of tuberculosis: comparison of immunoglobulin A (IgA) response to sulfolipid 1 with IgG and IgM responses to 2,3-diacyltrehalose 2,3,6-triacyltrehalose and cord factor antigens. J. Clin. Microbiol. **40:**3782–3788.
11. **Kawamura, M., N. Sueshige, K. Imayoshi, I. Yano, R. Maekura, and H. Kohno.** 1997. Enzyme immunoassay to detect antituberculous glycolipid antigen (anti-TBGL antigen) antibodies in serum for diagnosis of tuberculosis. J. Clin. Lab. Anal. **11:**140–145.
12. **Kishimoto, T., O. Moriya, J. Nakamura, T. Matsushima, and R. Soejima.** 1999. Evaluation of the usefulness of a serodiagnosis kit, the determiner TBGL antibody for tuberculosis: setting reference value. Kekkaku **74:**701–706.
13. **Kobayashi, J., and S. Kimura.** 1995. KL-6: a serum marker for interstitial pneumonia. Chest **108:**311–315.
14. **Maekura, R., M. Nakagawa, Y. Nakamura, T. Hiraga, Y. Yamamura, M. Ito, E. Ueda, S. Yano, H. He, and S. Oka.** 1993. Clinical evaluation of rapid serodiagnosis of pulmonary tuberculosis by ELISA with cord factor (trehalose-6,6′-dimycolate) as antigen purified from *Mycobacterium tuberculosis*. Am. Rev. Respir. Dis. **148:**997–1001.
15. **Maekura, R., Y. Okuda, M. Nakagawa, T. Hiraga, S. Yokota, M. Ito, I. Yano, H. Kohno, M. Wada, C. Abe, T. Toyoda, T. Kishimoto, and T. Ogura.** 2001. Clinical evaluation of anti-tuberculous glycolipid immunoglobulin G antibody assay for rapid serodiagnosis of pulmonary tuberculosis. J. Clin. Microbiol. **39:**3603–3608.
16. **Mazzei, G. J., M. D. Edgerton, C. Losberger, S. Lecoanet-Henchoz, P. Graber, A. Durandy, J. Gauchat, A. Bernard, B. Allet, and J. Bonnefoy.** 1995. Recombinant soluble trimetric CD40 ligand is biologically active. J. Biol. Chem. **31:** 7025–7028.
17. **Mempel, M., C. Ronet, F. Suarez, M. Gilleron, G. Puzo, L. V. Kaer, A. Lehuen, P. Kourilsky, and G. Gachelin.** 2002. Natural killer T cells restricted by the monomorphic MHC class 1b CD1d1 molecules behave like inflammatory cells. J. Immunol. **168:**365–371.
18. **Samten, B., E. K. Thomas, J. Gong, and P. F. Barnes.** 2000. Depressed CD40 ligand expression contributes to reduced gamma interferon production in human tuberculosis. Infect. Immun. **68:**3002–3006.
19. **Snyder-Cappione, J. E., D. F. Nixon, C. P. Loo, J. M. Chapman, D. A. Meiklejohn, F. F. Melo, P. R. Costa, J. K. Sandberg, D. S. Rodrigues, and E. G. Kallas.** 2007. Individuals with pulmonary tuberculosis have lower levels of circulating CD1d-restricted NKT cells. J. Infect. Dis. **195:**1361–1364.
20. **Vollmers, H. P., and S. Brändlein.** 2006. Natural IgM antibodies: from parias to parvenas. Histol. Histopathol. **21:**1355–1366.
21. **Wiley, J. A., R. Geha, and A. G. Harmsen.** 1997. Exogenous CD40 ligand induces a pulmonary inflammation response. J. Immunol. **158:**2932–2938.
22. **World Health Organization.** 2007. Global tuberculosis control: surveillance, planning, financing: WHO report 2007. World Health Organization, Geneva, Switzerland.
23. **Yarkoni, E., and H. J. Rapp.** 1977. Granuloma formation in lungs of mice after intravenous administration of emulsified trehalose-6,6′-dimycolate (cord factor): reaction intensity depends on size distribution of the oil droplets. Infect. Immun. **18:**552–554.
24. **Yu, W., E. Soprana, G. Cosentino, M. Volta, H. S. Lichenstein, G. Viale, and D. Vercelli.** 1998. Soluble $CD14_{1-152}$ confers responsiveness to both lipoarabinomannan and lipopolysaccharide in a novel HL-60 cell bioassay. J. Immunol. **161:**4244–4251.
25. **Zan, H., A. Cerutti, P. Dramitinos, A. Schaffer, and P. Casali.** 1998. CD40 engagement triggers switching to IgA1 and IgA2 in human B cells through induction of endogenous TGF-beta: evidence for TGF-beta but not IL-10-dependent direct S mu→S alpha and sequential S mu→S gamma S gamma→S alpha DNA recombination. J. Immunol. **161:**5217–5225.
26. **Zhang, Y., M. Doerfler, T. C. Lee, B. Guillemin, and W. N. Rom.** 1993. Mechanisms of stimulation of interleukin-1 beta and tumor necrosis factor-alpha by *Mycobacterium tuberculosis* components. J. Clin. Investig. **91:**2076–2083.